Quantum statistical-gauge geometry

Hai Pham-Van [*]

Department of Physics, Hanoi National University of Education, 136 Xuan Thuy, Cau Giay, Hanoi, Vietnam and Institute of Natural Sciences, Hanoi National University of Education, 136 Xuan Thuy, Cau Giay, Hanoi, Vietnam

(Received 26 December 2025; revised 5 May 2026; accepted 1 June 2026; published 16 June 2026)

Exact equilibrium constraints in quantum many-body systems, such as sum rules and Ward identities, can be hard to expose because local currents are distributional and equal-time commutators may contain anomaly-like contact terms. We present a simple geometric organization of the recently identified quantum shift symmetry. The local shifting superoperator is viewed as a statistical-gauge connection acting on observables, so hyperforces are covariant derivatives and force balance becomes a thermal Ward identity expressed with the Kubo-Mori inner product. For compact smearings we prove bulk flatness: smeared shift generators close on the Lie bracket of vector fields with no bulk Schwinger term. This closure yields an iterative, all-orders Ward-Bianchi hierarchy of equal-time constraints that closes on a finite set of force insertions and a bilinear force-gradient kernel, leading to general antisymmetry relations and positivity bounds. We fix the microscopic generator by quantizing the diffeomorphism moment map, where Weyl and half-density quantization agree and give a self-adjoint operator without bulk ordering anomalies. Although the bulk connection is flat, global topology remains through holonomy, which links naturally to twisted boundary conditions and flux threading. Background electromagnetic fields deform the algebra through explicit density-weighted curvature insertions rather than a bulk central extension. As an application we treat fractional quantum Hall fluids on a torus, connect the deformation to the guiding-center GMP-W_∞ algebra, and verify the key identities with exact diagonalization.

DOI: 10.1103/jb7b-rsfb

I. INTRODUCTION

Exact, nonperturbative identities—sum rules, Ward identities, and algebraic constraints—are among the sharpest pieces of information one can extract from an equilibrium many-body problem. They serve as internal consistency checks for analytic approximations, numerical solvers, and effective theories, and they often provide the only *a priori* constraints available at strong coupling. In equilibrium statistical mechanics this idea is intertwined with linear response: zero-frequency response coefficients are fixed by equal-time correlation functions and commutator structures, as emphasized in the classic developments of the fluctuation-dissipation relation and Kubo response theory [1–3] and in the Mori-Zwanzig projection formalism used to organize susceptibilities and memory kernels [4,5]. This response-theoretic viewpoint is naturally expressed through Kubo-Mori correlations and projection-operator dynamics [6–8]. From a modern perspective, these relations can be read as Ward-Takahashi-type statements for thermal expectation values, i.e., as identities implied by symmetries of the equilibrium state and its generating functional [8–11]. They are also complementary to recent studies of real-time many-body dynamics, where ultracold lattice systems have been used to probe equilibration, slow relaxation, and many-body localization in interacting disordered or quasiperiodic settings [12–15].

For classical fluids and soft-matter systems, force-balance, screening, and continuum constraints lead to exact structural restrictions on correlation functions, ranging from contact-value and compressibility-type relations to long-wavelength moment sum rules in Coulomb systems [16–19]. In inhomogeneous settings, closely related identities underlie density functional theory and integral equation approaches, where equilibrium correlations are constrained by variational principles and by the structure of the equilibrium measure [16,18]. These examples indicate a central theme of the present work: equilibrium itself already contains a large amount of hidden structure, but this structure may be obscured unless it is formulated in a way that makes its closure and iteration manifest.

A particularly transparent formulation has emerged recently for classical equilibrium. A series of works has shown that smooth coordinate deformations of the microscopic configuration variables act as statistical symmetries of the equilibrium measure, giving rise to Noether-like Ward relations for force and torque balance [20] and, crucially, to closed hierarchies of higher-order constraints on equal-time correlations [21–29]. In this viewpoint, the equilibrium Gibbs measure carries a gauge structure: hyperforce densities are the responses to local shifts, and the repeated application of shift Ward identities generates an "*ng*" tower of sum rules that terminates on a finite set of bulk insertions. A related gauge-geometric formulation unifies this gauge-shift invariance with conventional spacetime symmetries and organizes the resulting Noether and cross-Ward identities within a common Lie-algebraic structure [30]. This statistical-gauge interpretation has proven useful both conceptually and practically, e.g.,

[*]Contact author: haipv@hnue.edu.vn

as a set of stringent unit tests for simulation data and as a guide for constructing controlled approximations [31,32].

Extending such a statistical gauge symmetry to quantum equilibrium is, however, nontrivial. The obstacle is not merely technical. Local current generators are operator-valued distributions, and the equal-time algebra of conserved densities can acquire contact terms (Schwinger terms) that realize central extensions of the naive Lie algebra [33,34]. In relativistic quantum field theory, the interplay between current algebra, Ward identities, and anomalies is a textbook theme [9,10]; in nonrelativistic settings, closely related issues arise once one couples to curved or torsionful backgrounds or considers theories with Galilean and 't Hooft anomalies [35–37]. For our purposes, the key point is simple and sharp: a bulk central extension would obstruct the iterability of shift Ward identities, spoiling the closed "hierarchy" structure that makes the classical theory powerful.

At the same time, there is strong motivation to expect a geometric organization of quantum equilibrium constraints. First, quantum many-body systems admit a well-developed geometric coupling to external sources and spacetime backgrounds. For Galilean-invariant systems, coupling to Newton-Cartan structures and background gauge fields provides a systematic way to define and constrain the mass current, momentum density, and stress tensor, and to derive exact Ward identities for responses [38–40]. Second, in both relativistic and nonrelativistic hydrodynamics, equilibrium generating functionals impose powerful equality-type constraints on response data, without assuming weak coupling [41–43]. Finally, topology can enter equilibrium response through twisted boundary conditions and flux threading; in two dimensions, for instance, the Niu-Thouless-Wu formulation expresses quantized Hall response as a Berry-curvature integral over the twist torus, connecting flux insertion to geometric phases [44,45]. A quantum analog of the classical shift symmetry was recently identified by Müller and Schmidt [46] as a local shifting superoperator generated by the mass-current density, yielding an exact hyperforce balance identity in the Gibbs state. Here hyperforce denotes the generalized equilibrium force density associated with infinitesimal local relabelings of microscopic configuration variables. This immediately raises the central question of this work: does the quantum shift algebra close in the bulk without a Schwinger term, and what is the minimal structure that makes its closure and consequences transparent? We take the quantum hyperforce balance of Ref. [46] as the starting point. Our observation is geometric: the current-generated derivation defines a connection on the observable bundle, whose compactly supported bulk closure is the corresponding flatness condition, equivalently the Maurer-Cartan condition.

In this formulation, hyperforce balance becomes a covariant thermal Ward relation, and compactly supported smearings give bulk Lie closure of the shift algebra with no bulk Schwinger term. This closure yields an iterative equal-time Ward-Bianchi hierarchy that closes on a finite set of force insertions and a bilinear force-gradient kernel. The same connection viewpoint also organizes boundary corrections, holonomy, and background-field deformations. The underlying generator is fixed by quantization of the diffeomorphism moment map; Weyl and half-density quantizations agree and yield a self-adjoint operator free of bulk ordering anomalies.

Bulk flatness rules out local curvature obstructions but leaves global holonomy. On multiply connected manifolds, lift sectors are labeled by $U(1)$ characters, linking shift holonomy to twisted boundary conditions and flux threading. Coupling to background electromagnetic fields deforms closure through explicit density-weighted curvature insertions rather than a bulk central extension, separating flat-twist effects from genuine field strength.

We illustrate the construction for fractional quantum Hall fluids on the torus, where the magnetic deformation matches the guiding-center GMP-W_∞ algebra and organizes sector-resolved constraints under flux threading. Exact-diagonalization diagnostics provide direct checks of bulk closure, thermal Ward balance, and holonomy response on the twist torus.

The paper is organized as follows. Section II develops the statistical-gauge formulation of quantum shift symmetry, including bulk flatness, the closed Ward-Bianchi hierarchy, holonomy, and the background-field deformation. Section III applies the framework to fractional quantum Hall fluids on the torus. Section IV presents exact-diagonalization diagnostics. We conclude in Sec. V.

II. THEORETICAL CALCULATION

We first recall the quantum shift derivation and the exact hyperforce identity, then repackage the construction as a statistical-gauge connection whose distributional curvature controls closure, and finally derive the closed hierarchy together with its structural consequences (ordering, topology, and background-field deformations).

A. Shift symmetry and the hyperforce Ward identity

We recall local shift symmetry as a derivation acting on observables. Classically, it is generated by an infinitesimal canonical shift. In quantum equilibrium, the corresponding deformation is implemented as a commutator derivation generated by the mass-current density, defining the local shifting superoperator [46].

A natural formal issue is that this quantum construction is often presented as a direct implementation of Dirac's correspondence principle, replacing Poisson brackets by commutators. However, the Groenewold-van Hove theorem implies that no quantization map can preserve Poisson brackets for all phase-space polynomials [47–49]. This motivates examining which parts of the resulting hyperforce relations are quantization-independent, for example by comparing Weyl and geometric quantization. We show that three independent constructions of the shift generator-Weyl quantization, half-form geometric quantization, and moment-map quantization-agree identically. The argument uses two equivalent realizations of the same infinitesimal diffeomorphism generator: the Weyl calculus for momentum-linear symbols and the half-form representation in geometric quantization [50–52].

1. Shifting generator and local superoperator

Let M be the spatial domain, viewed as a smooth manifold possibly with boundary. Consider N particles with canonical phase-space variables $(\mathbf{r}_i, \mathbf{p}_i)$, where $\mathbf{r}_i \in M$ is the position of particle i and $\mathbf{p}_i$ is its canonical momentum. An infinitesimal shift by a smooth vector field $\boldsymbol{\epsilon}(\mathbf{r})$ is generated classically by

$$G_{\rm cl}[\boldsymbol{\epsilon}] = \sum_{i=1}^{N} \boldsymbol{\epsilon}(\mathbf{r}_i) \cdot \mathbf{p}_i. \tag{1}$$

The induced canonical variations are $\delta\mathbf{r}_i = \{\mathbf{r}_i, G_{\rm cl}\} = \boldsymbol{\epsilon}(\mathbf{r}_i)$ and $\delta\mathbf{p}_i = \{\mathbf{p}_i, G_{\rm cl}\} = -(\nabla_i \boldsymbol{\epsilon})^{\sf T} \cdot \mathbf{p}_i$. Here $\{\cdot,\cdot\}$ denotes the Poisson bracket on phase space, $\nabla_i \equiv \nabla_{\mathbf{r}_i}$ is the gradient with respect to $\mathbf{r}_i$, and ${}^{\sf T}$ denotes matrix transpose.

Quantum shifting gauge invariance is formulated most efficiently via the (operator-valued) local mass-current density $m\hat{\mathbf{J}}(\mathbf{r})$, with m the particle mass. For nonrelativistic particles (with momentum operators $\hat{\mathbf{p}}_i$ and position operators $\hat{\mathbf{r}}_i$) we use the standard symmetric operator-valued distribution

$$m\hat{\mathbf{J}}(\mathbf{r}) = \frac{1}{2}\sum_{i=1}^{N} (\hat{\mathbf{p}}_i\, \delta(\mathbf{r}-\hat{\mathbf{r}}_i) + \delta(\mathbf{r}-\hat{\mathbf{r}}_i)\, \hat{\mathbf{p}}_i), \tag{2}$$

where $\delta(\mathbf{r}-\hat{\mathbf{r}}_i)$ is the Dirac delta operator-valued distribution localized at the position operator $\hat{\mathbf{r}}_i$. The associated shifting superoperator is [46]

$$\boldsymbol{\sigma}(\mathbf{r}) \equiv -\frac{\rm i}{\hbar}[\,\cdot\,, m\hat{\mathbf{J}}(\mathbf{r})], \tag{3}$$

where $[\hat{A}, \hat{B}] = \hat{A}\hat{B} - \hat{B}\hat{A}$ is the commutator and $\hbar$ is the reduced Planck's constant. The map $\boldsymbol{\sigma}(\mathbf{r})$ sends operators to operators. For any observable $\hat{A}$ we define the (hyper)force density operator $\hat{\mathbf{S}}_A(\mathbf{r}) \equiv \boldsymbol{\sigma}(\mathbf{r})\hat{A}$ and the force density operator $\hat{\mathbf{F}}(\mathbf{r}) \equiv -\boldsymbol{\sigma}(\mathbf{r})\hat{H}$, where $\hat{H}$ is the many-body Hamiltonian. Throughout we take observables $\hat{A}$ to be Hermitian (self-adjoint), $\hat{A}^\dagger = \hat{A}$, unless stated otherwise.

In equilibrium we denote by $\hat{H}_0$ the Hamiltonian that defines the Gibbs state $\langle\cdot\rangle = {\rm Tr}\,(e^{-\beta\hat{H}_0}\cdot)/{\rm Tr}\,(e^{-\beta\hat{H}_0})$, with $\beta = (k_{\rm B}T)^{-1}$ the inverse temperature. Accordingly,

$$\hat{\mathbf{F}}_0(\mathbf{r}) = -\boldsymbol{\sigma}(\mathbf{r})\hat{H}_0. \tag{4}$$

The equilibrium hyperforce identity reads [46]

$$\mathbf{S}_A(\mathbf{r}) + (\hat{A}\,|\,\beta\hat{\mathbf{F}}_0(\mathbf{r})) = 0, \tag{5}$$

where $\mathbf{S}_A(\mathbf{r}) = \langle\hat{\mathbf{S}}_A(\mathbf{r})\rangle$ and $(\cdot|\cdot)$ is the Kubo-Mori (Bogoliubov) inner product,

$$(\hat{A}|\hat{B}) = \frac{1}{\beta}\int_0^\beta d\lambda\, \langle\hat{A}^\dagger\, e^{-\lambda\hat{H}_0}\hat{B}\, e^{\lambda\hat{H}_0}\rangle, \tag{6}$$

where $\hat{B}$ is an arbitrary self-adjoint observable, and $\lambda \in [0, \beta]$ is the imaginary-time parameter. Equation (5) is exact and holds for any observable $\hat{A}$ in equilibrium.

2. Weyl quantization

For a scalar one-body phase-space symbol $a(\mathbf{r}, \mathbf{p})$ [a smooth c-number function of position $\mathbf{r} \in \mathbb{R}^n$ and momentum $\mathbf{p} \in (\mathbb{R}^n)^*$ with sufficient decay], where n is the spatial dimension, its Weyl quantization ${\rm Op}_W(a)$ is defined by the integral kernel on $L^2(\mathbb{R}^n, d\mathbf{r})$, the Hilbert space of square-integrable wave functions $\psi : \mathbb{R}^n \to \mathbb{C}$ with respect to the Lebesgue measure $d\mathbf{r}$,

$$({\rm Op}_W(a)\psi)(\mathbf{r}) = \frac{1}{(2\pi\hbar)^n}\int d\mathbf{r}'\int d\mathbf{p}\, \exp\left(\frac{\rm i}{\hbar}\mathbf{p}\cdot(\mathbf{r}-\mathbf{r}')\right) \times a\left(\frac{\mathbf{r}+\mathbf{r}'}{2}, \mathbf{p}\right)\psi(\mathbf{r}'), \tag{7}$$

where $\psi(\mathbf{r})$ is the wave function evaluated at position $\mathbf{r}$ and $\mathbf{r}'$ is an integration variable.

For the momentum-linear symbol

$$a(\mathbf{r}, \mathbf{p}) = \mathbf{f}(\mathbf{r}) \cdot \mathbf{p}, \tag{8}$$

with $\mathbf{f}(\mathbf{r})$ a smooth vector field on $\mathbb{R}^n$, inserting Eq. (8) into Eq. (7) and integrating by parts yields

$$\begin{aligned}({\rm Op}_W(\mathbf{f}\cdot\mathbf{p})\psi)(\mathbf{r}) &= -{\rm i}\hbar\left[\mathbf{f}(\mathbf{r})\cdot\nabla + \tfrac{1}{2}(\nabla\cdot\mathbf{f}(\mathbf{r}))\right]\psi(\mathbf{r}) \\ &= \tfrac{1}{2}(\mathbf{f}(\hat{\mathbf{r}})\cdot\hat{\mathbf{p}} + \hat{\mathbf{p}}\cdot\mathbf{f}(\hat{\mathbf{r}}))\psi(\mathbf{r}),\end{aligned} \tag{9}$$

where $\hat{\mathbf{p}} = -{\rm i}\hbar\nabla$ and $\hat{\mathbf{r}}$ acts by multiplication. Equivalently,

$${\rm Op}_W(\mathbf{f}(\mathbf{r})\cdot\mathbf{p}) = \tfrac{1}{2}(\mathbf{f}(\hat{\mathbf{r}})\cdot\hat{\mathbf{p}} + \hat{\mathbf{p}}\cdot\mathbf{f}(\hat{\mathbf{r}})), \tag{10}$$

i.e., for symbols linear in momentum, Weyl quantization coincides with symmetric ordering.

Applying Eq. (10) to the classical shift generator (1) gives the Hermitian many-body Weyl generator

$$\begin{aligned}\hat{G}_W[\boldsymbol{\epsilon}] &= \sum_{i=1}^{N} {\rm Op}_W(\boldsymbol{\epsilon}(\mathbf{r}_i)\cdot\mathbf{p}_i) \\ &= \frac{1}{2}\sum_{i=1}^{N}(\boldsymbol{\epsilon}(\hat{\mathbf{r}}_i)\cdot\hat{\mathbf{p}}_i + \hat{\mathbf{p}}_i\cdot\boldsymbol{\epsilon}(\hat{\mathbf{r}}_i)),\end{aligned} \tag{11}$$

which implements the quantum shift by the commutator $\delta\hat{A} = ({\rm i}/\hbar)[\hat{G}_W[\boldsymbol{\epsilon}], \hat{A}]$.

The same midpoint rule fixes the quantum mass current. Classically, the one-body mass-current symbol is the distribution

$$m\mathbf{J}_{\rm cl}(\mathbf{r}) = \sum_i \mathbf{p}_i\, \delta(\mathbf{r}-\mathbf{r}_i),$$

i.e., the momentum density (times m) carried by point particles at $\mathbf{r}_i$. Smearing with a test vector field $\mathbf{u}(\mathbf{r})$ and using Eq. (10) yields

$$\int d\mathbf{r}\,\mathbf{u}(\mathbf{r})\cdot m\hat{\mathbf{J}}(\mathbf{r}) = \frac{1}{2}\sum_{i=1}^{N}(\mathbf{u}(\hat{\mathbf{r}}_i)\cdot\hat{\mathbf{p}}_i + \hat{\mathbf{p}}_i\cdot\mathbf{u}(\hat{\mathbf{r}}_i)). \tag{12}$$

By locality of the smearing, Eq. (12) is equivalent to the symmetric operator-valued distribution for $m\hat{\mathbf{J}}(\mathbf{r})$ given in Eq. (2). Hence the current entering the shifting superoperator (3) is precisely the Weyl-quantized mass-current density.

3. Geometric quantization

Geometric quantization provides an intrinsic route to the same shift generator that does not rely on the heuristic rule of replacing Poisson brackets by commutators. We sketch the argument in the simplest case $M = \mathbb{R}^n$, where the one-body phase space (the cotangent bundle of M) has canonical coordinates $(\mathbf{r}, \mathbf{p})$, canonical one-form $\vartheta = \mathbf{p}\cdot{\rm d}\mathbf{r}$, and symplectic form $\omega = \mathrm{d}\vartheta = \mathrm{d}\mathbf{p} \wedge \mathrm{d}\mathbf{r}$. Note that d denotes the exterior derivative, distinguished from d used for integration measures and ordinary derivatives.

Choosing the configuration (vertical) polarization means quantum states depend only on $\mathbf{r}$. With the metaplectic half-form correction, states are naturally treated as half-densities on M; concretely we work with the standard Schrödinger Hilbert space $L^2(\mathbb{R}^n, d\mathbf{r})$, but we remember that under a diffeomorphism $\varphi : \mathbb{R}^n \to \mathbb{R}^n$ the wave function transforms with a square-root Jacobian. The corresponding unitary action on half-densities is

$$(U_\varphi \psi)(\mathbf{r}) = \left|\det \frac{\partial \varphi^{-1}(\mathbf{r})}{\partial \mathbf{r}}\right|^{1/2} \psi(\varphi^{-1}(\mathbf{r})), \tag{13}$$

where $\partial\varphi^{-1}(\mathbf{r})/\partial\mathbf{r}$ is the Jacobian matrix of φ^{-1} at $\mathbf{r}$.

Let φ_t be the one-parameter flow generated by a smooth vector field $\boldsymbol{\epsilon}(\mathbf{r})$, with real parameter t,

$$\frac{d}{dt}\varphi_t(\mathbf{r}) = \boldsymbol{\epsilon}(\varphi_t(\mathbf{r})), \;\; \varphi_0(\mathbf{r}) = \mathbf{r}.$$

Differentiate Eq. (13) at $t = 0$. Using $\frac{d}{dt}|_0 \varphi_t^{-1}(\mathbf{r}) = -\boldsymbol{\epsilon}(\mathbf{r})$ and $\frac{d}{dt}|_0 \ln\det(\frac{\partial\varphi_t^{-1}(\mathbf{r})}{\partial\mathbf{r}}) = -\nabla\cdot\boldsymbol{\epsilon}(\mathbf{r})$ gives

$$\left.\frac{d}{dt}\right|_{t=0}(U_{\varphi_t}\psi)(\mathbf{r}) = -\boldsymbol{\epsilon}(\mathbf{r})\cdot\nabla\psi(\mathbf{r}) - \frac{1}{2}(\nabla\cdot\boldsymbol{\epsilon}(\mathbf{r}))\psi(\mathbf{r}). \tag{14}$$

In the operator formulas below, derivatives are understood by their action on a test wave function: $\boldsymbol{\epsilon}\cdot\nabla$ differentiates the wave function to its right, $(\nabla\cdot\boldsymbol{\epsilon})(\mathbf{r})$ and $(\nabla\cdot\boldsymbol{\epsilon})(\mathbf{r}_i)$ act by scalar multiplication, and $\hat{\mathbf{p}}_i\cdot\boldsymbol{\epsilon}(\hat{\mathbf{r}}_i) \equiv -\mathrm{i}\hbar\,\nabla_i\cdot[\boldsymbol{\epsilon}(\mathbf{r}_i)\,\cdot\,]$. Therefore the quantum generator of the diffeomorphism flow is

$$\begin{aligned}\hat{q}[\boldsymbol{\epsilon}] &= \mathrm{i}\hbar \left.\frac{d}{dt}\right|_{t=0} U_{\varphi_t}\\ &= -\mathrm{i}\hbar\Big(\boldsymbol{\epsilon}(\mathbf{r})\cdot\nabla + \frac{1}{2}\,\nabla\cdot\boldsymbol{\epsilon}(\mathbf{r})\Big) = -\mathrm{i}\hbar\,\mathcal{L}_{\boldsymbol{\epsilon}}^{(1/2)},\end{aligned} \tag{15}$$

where $\mathcal{L}_{\boldsymbol{\epsilon}}^{(1/2)}$ is the Lie derivative on half-densities.

For N particles, the geometric-quantization generator is the sum over particles, $\hat{G}_{\mathrm{GQ}}[\boldsymbol{\epsilon}] = \sum_{i=1}^N \hat{q}^{(i)}[\boldsymbol{\epsilon}]$,

$$\hat{G}_{\mathrm{GQ}}[\boldsymbol{\epsilon}] = -\mathrm{i}\hbar\sum_{i=1}^N \Big(\boldsymbol{\epsilon}(\mathbf{r}_i)\cdot\nabla_i + \frac{1}{2}\nabla_i\cdot\boldsymbol{\epsilon}(\mathbf{r}_i)\Big), \tag{16}$$

We can rewrite the one-particle operator in the familiar symmetric form:

$$\begin{aligned}&\tfrac{1}{2}(\boldsymbol{\epsilon}(\hat{\mathbf{r}}_i)\cdot\hat{\mathbf{p}}_i + \hat{\mathbf{p}}_i\cdot\boldsymbol{\epsilon}(\hat{\mathbf{r}}_i))\\ &\quad= \tfrac{1}{2}[\boldsymbol{\epsilon}(\mathbf{r}_i)\cdot(-\mathrm{i}\hbar\nabla_i) + (-\mathrm{i}\hbar\nabla_i)\cdot\boldsymbol{\epsilon}(\mathbf{r}_i)]\\ &\quad= -\mathrm{i}\hbar\big(\boldsymbol{\epsilon}(\mathbf{r}_i)\cdot\nabla_i + \tfrac{1}{2}\,\nabla_i\cdot\boldsymbol{\epsilon}(\mathbf{r}_i)\big).\end{aligned} \tag{17}$$

Summing over i yields $\hat{G}_{\mathrm{GQ}}[\boldsymbol{\epsilon}] = \hat{G}_W[\boldsymbol{\epsilon}]$ [Eq. (11)]. Thus geometric quantization (with the half-form correction) reproduces the same Hermitian generator as Weyl quantization for momentum-linear symbols, and consequently leads to the same symmetrized current density $m\hat{\mathbf{J}}(\mathbf{r})$ in Eq. (2).

B. Statistical-gauge geometry and bulk flatness

With the local shift derivation in place, we now recast it in geometric language [53–55]. Write the shift superoperator as a derivation-valued vector $\boldsymbol{\sigma}(\mathbf{r}) = (\sigma_1(\mathbf{r}), \sigma_2(\mathbf{r}), \sigma_3(\mathbf{r}))$. Introduce the canonical $\mathbb{R}^3$-valued soldering one-form ϖ on M, defined by $\varpi_{\mathbf{r}}(\mathbf{u}) = \mathbf{u}$. Denote $T_{\mathbf{r}}M$ as the tangent space of M at the point $\mathbf{r}$, and let $\mathbf{u} \in T_{\mathbf{r}}M$ be a tangent vector representing an infinitesimal displacement at $\mathbf{r}$. Form the derivation-valued connection one-form Γ by contraction,

$$\Gamma = \boldsymbol{\sigma}(\mathbf{r})\cdot\varpi, \;\; \Gamma_{\mathbf{r}}(\mathbf{u}) = \boldsymbol{\sigma}(\mathbf{r})\cdot\mathbf{u}. \tag{18}$$

The coefficients $\sigma_i(\mathbf{r})$ are the components of Γ in a local coframe on M. Let $\mathfrak{A}_{\mathrm{obs}}$ be the unital $*$-algebra of observables, represented on the many-body Hilbert space $\mathcal{H}$. Let $\mathcal{A}(\mathbf{r})$ be an operator-valued field, that is a section of the trivial operator bundle $E = M\times\mathfrak{A}_{\mathrm{obs}} \to M$, whose fiber over each $\mathbf{r}\in M$ is the same observable algebra $\mathfrak{A}_{\mathrm{obs}}$. Define the covariant exterior derivative operator by

$$D = \mathrm{d} + \Gamma. \tag{19}$$

Its action on an operator-valued field $\mathcal{A}(\mathbf{r})$ is $D\mathcal{A} = \mathrm{d}\mathcal{A} + \Gamma\,\mathcal{A}$. For a base-constant section $\mathcal{A}(\mathbf{r}) \equiv \hat{A}$, this reduces to $D\mathcal{A} = \Gamma\,\hat{A}$, which reproduces the local hyperforce action.

The curvature is the corresponding derivation-valued two-form

$$\mathcal{F} = D^2 = \mathrm{d}\Gamma + \Gamma\wedge\Gamma, \tag{20}$$

where $\wedge$ is the exterior wedge product of differential forms on M. For tangent vectors $\mathbf{u}, \mathbf{v} \in T_{\mathbf{r}}M$ one has

$$(\Gamma\wedge\Gamma)(\mathbf{u},\mathbf{v}) = [\Gamma(\mathbf{u}), \Gamma(\mathbf{v})].$$

For compactly supported vector fields $\mathbf{f}, \mathbf{g} \in C_c^\infty(M, \mathbb{R}^3)$ define the directional covariant derivatives by

$$D_{\mathbf{f}}\mathcal{A} = (D\mathcal{A})(\mathbf{f}) = (\mathrm{d}\mathcal{A})(\mathbf{f}) + \Gamma(\mathbf{f})\,\mathcal{A}, \;\; \Gamma(\mathbf{f}) = \Gamma_{\mathbf{r}}(\mathbf{f}_{\mathbf{r}}).$$

Then the curvature measures the failure of covariant Lie closure via

$$\mathcal{F}(\mathbf{f},\mathbf{g}) = [D_{\mathbf{f}}, D_{\mathbf{g}}] - D_{[\mathbf{f},\mathbf{g}]}.$$

In the bulk, the distributional kernel implies the covariant Lie identity. Here and below the Lie bracket of vector fields is defined as $[\mathbf{f},\mathbf{g}] = (\mathbf{f}\cdot\nabla)\mathbf{g} - (\mathbf{g}\cdot\nabla)\mathbf{f}$:

$$[D_{\mathbf{f}}, D_{\mathbf{g}}] = D_{[\mathbf{f},\mathbf{g}]} \;\text{bulk}, \tag{21}$$

and hence $\mathcal{F} = 0$ distributionally. More explicitly, compactly supported $\mathbf{f}$ and $\mathbf{g}$ test only the interior distributional kernel, so Eq. (21) states that $\mathcal{F}(\mathbf{f},\mathbf{g}) = 0$ for all bulk test fields. This is the local flatness statement of the statistical connection: successive shift variations close on $[\mathbf{f},\mathbf{g}]$ without producing any additional bulk insertion. Possible failures of closure are therefore confined to boundary terms, displayed below, or to the background-field curvature introduced in Sec. II F.

For a base-constant observable section $\mathcal{A}(\mathbf{r}) \equiv \hat{A}$, the smeared action of the directional covariant derivative is exactly the smeared shifting derivation,

$$\int_M d\mathbf{r}\,(D\mathcal{A})_{\mathbf{r}}(\mathbf{f}_{\mathbf{r}}) = \int_M d\mathbf{r}\,\mathbf{f}(\mathbf{r})\cdot\boldsymbol{\sigma}(\mathbf{r})\hat{A} = \Sigma[\mathbf{f}]\hat{A}. \tag{22}$$

Thus Eq. (21) is the compact-support closure relation written in $D_{\mathbf{f}}$ notation, while $\Sigma[\mathbf{f}]$ is the same shift action after smearing over M.

The operator-valued one-form representation used next is an alternative inner representation of the same connection, not a redefinition. Define

$$\Omega_{\mathbf{r}}(\mathbf{u}) = -\frac{\mathrm{i}}{\hbar}\,m\hat{\mathbf{J}}(\mathbf{r})\cdot\mathbf{u},\quad \Gamma(\mathbf{u}) = \mathrm{ad}_{\Omega(\mathbf{u})}, \tag{23}$$

meaning $\mathrm{ad}_{\Omega(\mathbf{u})}X = [X,\Omega(\mathbf{u})]$ for any $X\in\mathfrak{A}_{\mathrm{obs}}$. Indeed,

$$\Gamma_{\mathbf{r}}(\mathbf{u})X = [X, -(\mathrm{i}/\hbar)m\hat{\mathbf{J}}(\mathbf{r})\cdot\mathbf{u}] = (\boldsymbol{\sigma}(\mathbf{r})\cdot\mathbf{u})X,$$

so this is precisely the action of $\Gamma_{\mathbf{r}}(\mathbf{u})$ defined in Eq. (18). With this right-adjoint convention, the curvature can be written as

$$\mathcal{F} = \mathrm{ad}_{\mathcal{K}_\Omega},\quad \mathcal{K}_\Omega = \mathrm{d}\Omega - \Omega\wedge\Omega, \tag{24}$$

where $(\Omega\wedge\Omega)(\mathbf{u},\mathbf{v}) = [\Omega(\mathbf{u}),\Omega(\mathbf{v})]$ and $\mathrm{ad}_{\mathcal{K}_\Omega}(\mathbf{u},\mathbf{v})X = [X,\mathcal{K}_\Omega(\mathbf{u},\mathbf{v})]$. Hence Eq. (21) is equivalent to $\mathrm{ad}_{\mathcal{K}_\Omega}=0$. A nonzero $\mathcal{K}_\Omega$ would have to be central; since no bulk Schwinger term is present for compactly supported smearings, as justified below in Sec. II D, the same flatness condition becomes the Maurer-Cartan equation [53]

$$\mathrm{d}\Omega - \Omega\wedge\Omega = 0\ \text{bulk}. \tag{25}$$

Thus the covariant Lie identity and the Maurer-Cartan equation are the same bulk-flatness condition written, respectively, in covariant-derivative and inner-one-form language.

These relations provide the geometric backbone of the shift symmetry in the quantum many-body setting. Equation (19) identifies Γ as a statistical connection on the observable bundle, so that local shift responses are encoded as covariant derivatives. The bulk identity in Eq. (21) is the key structural statement: it expresses distributional flatness of the connection and guarantees that successive shift variations close on the Lie bracket without generating additional bulk terms. As a consequence, Ward identities derived from the hyperforce balance can be iterated consistently to all orders, leading to a closed hierarchy of equal-time constraints. The Maurer-Cartan form of flatness makes the absence of bulk anomalies transparent and cleanly separates bulk physics from possible boundary contributions, which may enter only through noncompact smearings or boundary conditions.

If M has a boundary ∂M, the bulk flatness statement remains valid for compactly supported smearings, but for general smooth vector fields the distributional integration by parts produces a boundary refinement of the smeared closure. Writing the smeared shift generator as $\Sigma[\mathbf{f}] = \int_M d\mathbf{r}\,\mathbf{f}(\mathbf{r})\cdot\boldsymbol{\sigma}(\mathbf{r})$, one finds the boundary version

$$[\Sigma[\mathbf{f}],\Sigma[\mathbf{g}]] = \Sigma[[\mathbf{f},\mathbf{g}]] + \int_{\partial M} dS\,[(\mathbf{n}\cdot\mathbf{g})\mathbf{f} - (\mathbf{n}\cdot\mathbf{f})\mathbf{g}]\cdot\boldsymbol{\sigma}(\mathbf{r}), \tag{26}$$

where dS is the surface measure on ∂M and $\mathbf{n}$ is the outward unit normal. Equation (26) is the same closure statement written in the equivalent smeared-superoperator notation, but now for vector fields that need not have compact support. The boundary correction may be denoted

$$B_\partial[\mathbf{f},\mathbf{g}] = \int_{\partial M} dS\,[(\mathbf{n}\cdot\mathbf{g})\mathbf{f} - (\mathbf{n}\cdot\mathbf{f})\mathbf{g}]\cdot\boldsymbol{\sigma}(\mathbf{r}), \tag{27}$$

so that, on base-constant observable sections,

$$[\Sigma[\mathbf{f}],\Sigma[\mathbf{g}]]\hat{A} = \Sigma[[\mathbf{f},\mathbf{g}]]\hat{A} + B_\partial[\mathbf{f},\mathbf{g}]\hat{A}. \tag{28}$$

For compactly supported smearings, $B_\partial[\mathbf{f},\mathbf{g}]=0$, and Eq. (26) reduces exactly to Eq. (21). The same reduction holds for boundary-preserving vector fields satisfying $\mathbf{n}\cdot\mathbf{f} = \mathbf{n}\cdot\mathbf{g} = 0$ on ∂M. Consequently, the Ward-Bianchi hierarchy closes purely on bulk insertions only for boundary-preserving smearings, such as $\mathbf{f}\in C_c^\infty(M,\mathbb{R}^3)$ or $\mathbf{n}\cdot\mathbf{f}|_{\partial M}=0$; otherwise the surface term in Eq. (26) generates additional ∂M-supported insertions at each iteration.

C. All-orders closed Ward-Bianchi hierarchy

We next turn the geometric structure into concrete, testable equilibrium constraints. Using $D_{\mathbf{f}}\hat{A} = \Sigma[\mathbf{f}]\hat{A}$ for base-constant observable sections, the bulk flatness relation in Eq. (21) becomes the following smeared-superoperator closure for compactly supported smearings:

$$[\Sigma[\mathbf{f}],\Sigma[\mathbf{g}]] = \Sigma[[\mathbf{f},\mathbf{g}]]. \tag{29}$$

Thus Eq. (29) is Eq. (21) written in smeared-shift notation, while Eq. (26) is its boundary-refined version. The same smeared shifting derivation defines the dimensionless force insertion

$$F[\mathbf{f}] = \int_M d\mathbf{r}\,\mathbf{f}(\mathbf{r})\cdot\beta\hat{\mathbf{F}}_0(\mathbf{r}) = -\Sigma[\mathbf{f}]\,\beta\hat{H}_0, \tag{30}$$

and the bilinear force-gradient kernel

$$K_0[\mathbf{f},\mathbf{g}] = \Sigma[\mathbf{f}]F[\mathbf{g}] = -\Sigma[\mathbf{f}]\Sigma[\mathbf{g}]\,\beta\hat{H}_0. \tag{31}$$

Applying the smeared Ward identity $\langle\Sigma[\mathbf{f}]\hat{A}\rangle + (\hat{A}|F[\mathbf{f}]) = 0$ to $\hat{A} = \prod_{j=1}^{n-1}F[\mathbf{f}_j]$ and using the Leibniz product rule gives, for all $n\geqslant 2$,

$$\left(\prod_{j=1}^{n-1}F[\mathbf{f}_j]\,\middle|\,F[\mathbf{f}_n]\right) + \sum_{k=1}^{n-1}\left\langle\left(\prod_{j<k}F[\mathbf{f}_j]\right)\times K_0[\mathbf{f}_n,\mathbf{f}_k]\left(\prod_{j>k}F[\mathbf{f}_j]\right)\right\rangle = 0. \tag{32}$$

Equation (32) is the nth member of the closed equal-time Ward hierarchy. It provides an exact n-point constraint on smeared force insertions and can be viewed as an ng-sum rule in direct analogy with the classical ng relations for higher-order equilibrium correlations.

The insertions in Eq. (32) have a direct interpretation as static force-density moments. The object $F[\mathbf{f}]$ is a smeared microscopic force density, while K_0 is the associated force-stiffness kernel. In real space,

$$K_0[\mathbf{f},\mathbf{g}] = \int_M d\mathbf{r}\,d\mathbf{r}'\,f_\alpha(\mathbf{r})g_\beta(\mathbf{r}')K^{(2)}_{\alpha\beta}(\mathbf{r},\mathbf{r}'),$$
$$K^{(2)}_{\alpha\beta}(\mathbf{r},\mathbf{r}') \equiv \sigma_\alpha(\mathbf{r})[\beta\hat{\mathbf{F}}_{0,\beta}(\mathbf{r}')]. \tag{33}$$

Thus $K^{(2)}$ measures the equal-time linear variation of the β component of the force density at $\mathbf{r}'$ produced by a local displacement near $\mathbf{r}$; higher force gradients are successive local force-stiffnesses. The $n=2$ member, $(F[\mathbf{f}]|F[\mathbf{g}]) = -\langle K_0[\mathbf{g},\mathbf{f}]\rangle$, is therefore the quantum force-fluctuation-force-gradient sum rule. The connection to ordinary density correlations follows by taking $\hat{A} = \prod_{a=1}^{m}\hat{\rho}(\mathbf{r}_a)$ in the basic Ward identity. Since $\Sigma[\mathbf{f}]\hat{\rho}(\mathbf{r}) = -\nabla\cdot[\mathbf{f}(\mathbf{r})\hat{\rho}(\mathbf{r})]$, one obtains, up to the standard coincident-point contact terms,

$$\left(\prod_{a=1}^{m}\hat{\rho}(\mathbf{r}_a)\mid F[\mathbf{f}]\right) = \sum_{a=1}^{m}\nabla_a\cdot[\mathbf{f}(\mathbf{r}_a)G_m(\mathbf{r}_1,\dots,\mathbf{r}_m)],$$
$$G_m(\mathbf{r}_1,\dots,\mathbf{r}_m) = \left\langle\prod_{a=1}^{m}\hat{\rho}(\mathbf{r}_a)\right\rangle. \tag{34}$$

Higher members of Eq. (32) therefore convert additional force insertions into force-gradient kernels and yield exact moment constraints on multipoint density correlations, in direct analogy with the Yvon-Born-Green and moment-sum-rule constraints of standard liquid-state theory [16,19].

This tower closes on F and K_0 and generates no new bulk insertions at higher order. Flatness and Lie closure further enforce Bianchi-type compatibility. In particular,

$$K_0[\mathbf{f},\mathbf{g}] - K_0[\mathbf{g},\mathbf{f}] = F[[\mathbf{f},\mathbf{g}]]. \tag{35}$$

Moreover, Mori positivity yields the stability bound

$$(F[\mathbf{f}]\mid F[\mathbf{f}]) = -\langle K_0[\mathbf{f},\mathbf{f}]\rangle \geqslant 0. \tag{36}$$

Equations (32)–(36) constitute the closed set of bulk equal-time constraints implied by shift symmetry in the flat case. To make clear why this closure is consistent in the quantum theory, we next explain how operator ordering and the derivation property exclude bulk Schwinger terms and central extensions.

D. First-principles ordering and absence of bulk anomalies

The hierarchy above hinges on two structural inputs: (i) $\Sigma[\mathbf{f}]$ acts as a derivation on a unital observable algebra, and (ii) the Lie closure (29) holds without bulk corrections. We now justify these statements from complementary viewpoints: an algebraic argument excluding central extensions and a microscopic quantization argument fixing the generator ordering.

For compactly supported smearings $\mathbf{f},\mathbf{g}\in C_c^\infty(M,\mathbb{R}^3)$, the smeared shift generator $\Sigma[\mathbf{f}]$ acts as a derivation on the unital observable algebra $\mathfrak{A}_{\text{obs}}$. Therefore the commutator $[\Sigma[\mathbf{f}],\Sigma[\mathbf{g}]]$ is again a derivation. A genuine bulk Schwinger term would be proportional to the identity superoperator and hence cannot satisfy the Leibniz product rule on a unital algebra. This excludes a bulk central extension and is consistent with the distributional flatness statement in Eq. (21).

Microscopically, the shift generator is fixed by quantizing the classical diffeomorphism moment map, i.e., the momentum-linear shift symbol underlying the classical generator in Eq. (1). As shown in Sec. II A 2, Weyl quantization yields the unique self-adjoint many-body generator $\hat{Q}[\boldsymbol{\epsilon}] \equiv \hat{G}_W[\boldsymbol{\epsilon}]$ in Eq. (11). Equivalently, geometric quantization with the metaplectic (half-form) correction produces the same operator, $\hat{G}_{\text{GQ}}[\boldsymbol{\epsilon}]$ in Eq. (16). With this choice, the local mass current entering the shifting superoperator in Eq. (3) is the corresponding symmetrized current density in Eq. (2).

Because the underlying symbol is fiber-linear in momentum, the Groenewold-Moyal expansion [56] truncates, so the generator algebra closes exactly with no $\hbar^2$ ordering anomaly:

$$\frac{\mathrm{i}}{\hbar}[\hat{Q}[\boldsymbol{\epsilon}_1],\hat{Q}[\boldsymbol{\epsilon}_2]] = \hat{Q}[[\boldsymbol{\epsilon}_1,\boldsymbol{\epsilon}_2]], \tag{37}$$

where $[\boldsymbol{\epsilon}_1,\boldsymbol{\epsilon}_2]$ is the Lie bracket of vector fields on M. Passing to adjoint actions, $\Sigma[\boldsymbol{\epsilon}] = -(\mathrm{i}/\hbar)\,\mathrm{ad}_{\hat{Q}[\boldsymbol{\epsilon}]}$, this implies the bulk superoperator closure in Eq. (29).

If M has a boundary or one uses noncompact smearings, the only additional contributions are boundary cocycles generated by integration by parts, as in Eq. (26). These terms are inner and may be removed or controlled by boundary-preserving smearings or by appropriate boundary conditions and counterterms. The bulk algebra remains anomaly-free.

Having fixed a self-adjoint generator and excluded bulk central extensions, we can treat the bulk hierarchy as exact. The remaining subtlety is global rather than local: even a flat connection can have nontrivial holonomy on multiply connected M. We therefore turn to the topology encoded by holonomy sectors next.

E. Topology from holonomy: Lift sectors, twisted traces, and selection rules

Flatness removes local curvature invariants but not global structure. The topological data discussed here are therefore distinct from the bulk-flatness condition of Sec. II B and from the closed Ward-Bianchi constraints of Sec. II C. They are global holonomies of the same flat statistical connection, not additional bulk-curvature terms. They are also distinct from the background-field curvature deformation of Sec. II F; on a torus they are implemented as flat twist phases or boundary-condition phases. We use standard facts about flat connections, holonomy, and first cohomology with $U(1)$ coefficients [54,57,58]. For a closed loop $\gamma\subset M$ we define the Wilson operator U_γ as the path-ordered exponential of the mass-current one-form integrated along γ,

$$U_\gamma = \mathcal{P}\exp\left(-\frac{\mathrm{i}}{\hbar}\oint_\gamma m\hat{\mathbf{J}}(\mathbf{r})\cdot d\mathbf{r}\right),\quad \mathcal{W}[\gamma] = \mathrm{Ad}_{U_\gamma}, \tag{38}$$

where $\mathcal{P}$ denotes path ordering along γ and Ad_{U_γ} is the adjoint action on observables, defined by $\mathrm{Ad}_{U_\gamma}(X) = U_\gamma X U_\gamma^{-1}$ for any $X\in\mathfrak{A}_{\text{obs}}$. In the bulk, the induced automorphism $\mathcal{W}[\gamma]$ depends only on the homotopy class $[\gamma]$ in the fundamental group $\pi_1(M)$, the group of loop classes under concatenation.

Because the connection is ad-valued, U_γ is defined only up to multiplication by a central phase in $U(1)$, the group of complex numbers of unit modulus. Equivalently, the adjoint holonomy fixes the unitary lift only projectively; two lifts of the same adjoint holonomy may differ by a phase that is multiplicative under loop concatenation. Inequivalent lifts are therefore classified by a character χ, namely, a group homomorphism $\chi:\pi_1(M)\to U(1)$. Since $U(1)$ is Abelian, every such character factors through the Abelianization of the fundamental group, $H_1(M;\mathbb{Z})\simeq\pi_1(M)_{\text{ab}}$. The universal coefficient theorem then identifies these characters with the first cohomology group with constant $U(1)$ coefficients [57,58]:

$$\begin{aligned}\chi &\in \mathrm{Hom}(\pi_1(M), U(1)),\\ \mathrm{Hom}(\pi_1(M), U(1)) &\simeq \mathrm{Hom}(H_1(M;\mathbb{Z}), U(1))\\ &\simeq H^1(M;U(1)).\end{aligned} \tag{39}$$

Here $H^1(M;U(1))$ is the first cohomology group of M with coefficients in the unitary Abelian group $U(1)$.

A practical thermal probe is the Wilson character

$$W_\gamma(\beta) = \frac{\mathrm{Tr}\,(e^{-\beta\hat{H}_0}U_\gamma)}{\mathrm{Tr}\,(e^{-\beta\hat{H}_0})} = \langle U_\gamma\rangle_\beta,\ \ \Phi_\gamma(\beta) = \arg W_\gamma(\beta), \tag{40}$$

where $\Phi_\gamma(\beta)$ is the phase of the thermal Wilson character.

Large transformations φ also define twisted traces, with U_φ the unitary implementing φ on the many-body Hilbert space $\mathcal{H}$, and the corresponding twisted partition function

$$Z_\varphi(\beta) = \mathrm{Tr}\,(e^{-\beta\hat{H}_0}U_\varphi).$$

For $M = \mathbb{T}^n$, one has $\pi_1(\mathbb{T}^n) = \mathbb{Z}^n$ and hence $H^1(\mathbb{T}^n;U(1)) \simeq U(1)^n$. A character is therefore specified by n phases $\chi(e_j) = e^{\mathrm{i}\theta_j}$, one for each fundamental cycle. This is the cohomological origin of the twist angles. On the n-dimensional torus $M = \mathbb{T}^n$, a twist sector $\boldsymbol{\theta} \in [0, 2\pi)^n$ shifts momentum quantization. In the jth direction, the allowed total momentum eigenvalues P_j are shifted as

$$P_j = \frac{\hbar}{L_j}(2\pi m_j + N\theta_j),$$

where L_j is the system size along direction j, $m_j \in \mathbb{Z}$ is an integer mode label, N is the total particle number, and θ_j is the twist angle.

Holonomy also grades observables: if $\pi_1(M)$ is Abelian and the Kubo-Martin-Schwinger (KMS) state is monodromy-invariant, then an observable A in a nontrivial character sector satisfies $\langle A\rangle_\beta = 0$, and a nonzero correlator $\langle\prod_\ell A_\ell\rangle_\beta \neq 0$ requires the product of the corresponding characters to be trivial.

As a discrete illustration, consider a Hubbard ring with twist θ. Let $\hat{\mathcal{T}}$ denote the lattice translation operator by one site and let L be the number of sites, so that $\hat{\mathcal{T}}^L$ is the translation around one full loop. In a fixed-N sector one has $U_\gamma \simeq \hat{\mathcal{T}}^L = e^{\mathrm{i}N\theta}\mathbb{1}$, and hence $\Phi_\gamma(\beta) = N\theta \pmod{2\pi}$.

These holonomy relations are the global counterpart of the bulk Ward-Bianchi constraints discussed above. Even when the statistical connection is flat in the bulk, nontrivial loop holonomies U_γ can survive and label inequivalent lift sectors by the first cohomology group $H^1(M;U(1))$. The thermal Wilson character $W_\gamma(\beta)$ and the twisted trace $Z_\varphi(\beta)$ provide practical, computable probes of these sectors, while the associated character grading imposes sharp selection rules on equilibrium one- and many-point functions. In this way, topology supplies exact, nonperturbative constraints that complement the local Ward identities, and it offers a clean diagnostic for twisted boundary conditions and flux insertion in analytic work and numerics.

F. Curved generalizations

We separate metric curvature from statistical-gauge curvature. The "bulk flatness" used above indicates flatness of the shift connection, not flatness of the background spatial metric. On a fixed Riemannian manifold (M, g) the Hermitian shift generator is the half-density Lie derivative, $\hat{G}_g[\mathbf{f}] = -\mathrm{i}\hbar\sum_a[f^i(\hat{\mathbf{r}}_a)\nabla_{ai} + \frac{1}{2}(\nabla_i f^i)(\hat{\mathbf{r}}_a)]$, with $\nabla_i f^i$ the Levi-Civita divergence. Since half-density Lie derivatives obey $[\mathcal{L}^{1/2}_{\mathbf{f}}, \mathcal{L}^{1/2}_{\mathbf{g}}] = \mathcal{L}^{1/2}_{[\mathbf{f},\mathbf{g}]}$, compact smearings satisfy $(\mathrm{i}/\hbar)[\hat{G}_g[\mathbf{f}], \hat{G}_g[\mathbf{g}]] = \hat{G}_g[[\mathbf{f},\mathbf{g}]]$ with no term proportional to the identity. Thus Riemann curvature may enter $\hat{H}_0$, the force insertions, and stress responses through covariant derivatives and possible curvature couplings, but it does not generate a bulk central charge or spoil the Ward-Bianchi iteration. For example, on the Haldane sphere the Gaussian curvature of S^2 only covariantizes the generator; the algebraic deformation comes from the monopole $U(1)$ field strength, which is the electromagnetic curvature treated below.

We next turn to gauge-field curvature by coupling the system to a fixed background electromagnetic field. The key conceptual point is that the resulting deformation of the shift algebra is inner (it acts by commutator with a density-weighted field-strength insertion) and therefore preserves the Leibniz product rule, rather than producing a bulk central extension that would obstruct the Ward-Bianchi iteration.

Minimal coupling replaces the canonical momentum operator $\hat{\mathbf{p}}$ by the covariant kinetic momentum $\hat{\boldsymbol{\pi}}$:

$$\hat{\boldsymbol{\pi}} = \hat{\mathbf{p}} - q\,\mathbf{A}(\hat{\mathbf{r}}),$$

where q is the particle charge, $\hat{\mathbf{r}}$ is the position operator, and $\mathbf{A}(\hat{\mathbf{r}})$ is the vector potential evaluated at $\hat{\mathbf{r}}$. Because the covariant momenta do not commute in a magnetic field, their algebra generates a genuine curvature insertion rather than a central extension.

For smooth smearings $\mathbf{f}$ and $\mathbf{g}$, define $\hat{G}_{\mathbf{A}}[\mathbf{f}]$ by the minimal-coupling replacement $\hat{\mathbf{p}} \to \hat{\boldsymbol{\pi}}$ in the many-body half-density generator, and set $\Sigma_{\mathbf{A}}[\mathbf{f}] = -(\mathrm{i}/\hbar)\,\mathrm{ad}_{\hat{G}_{\mathbf{A}}[\mathbf{f}]}$. A direct commutator calculation yields

$$\begin{aligned}[\hat{G}_{\mathbf{A}}[\mathbf{f}], \hat{G}_{\mathbf{A}}[\mathbf{g}]] = &-\mathrm{i}\hbar\,\hat{G}_{\mathbf{A}}[[\mathbf{f},\mathbf{g}]] + \mathrm{i}\hbar\,q\\ &\times\int d\mathbf{r}\,\big(f^i g^j F^{\mathrm{em}}_{ij}\big)(\mathbf{r})\,\hat{\rho}(\mathbf{r}),\end{aligned} \tag{41}$$

where $F^{\mathrm{em}}_{ij}(\mathbf{r}) = \partial_i A_j(\mathbf{r}) - \partial_j A_i(\mathbf{r})$ is the electromagnetic field-strength tensor and $\hat{\rho}(\mathbf{r}) = \sum_a\delta(\mathbf{r} - \hat{\mathbf{r}}_a)$ is the microscopic particle-density operator. Throughout, repeated spatial component indices, such as i, j in $f^i g^j F^{\mathrm{em}}_{ij}$, are summed over (Einstein convention), whereas particle, orbital, mode, and spectral labels are not summed unless explicitly indicated.

The second term in Eq. (41) is an inner cocycle proportional to the density, so the induced statistical curvature acts on any observable $X \in \mathfrak{A}_{\mathrm{obs}}$ by commutation with $qF^{\mathrm{em}}\hat{\rho}$,

$$\mathcal{F}^{(\mathbf{A})}_{ij}(\mathbf{r})[X] = \frac{\mathrm{i}}{\hbar}\big[X,\ qF^{\mathrm{em}}_{ij}(\mathbf{r})\hat{\rho}(\mathbf{r})\big].$$

Thus background gauge fields deform the Ward-Bianchi structure through explicit curvature insertions and flux-sensitive holonomy, rather than through a bulk central extension.

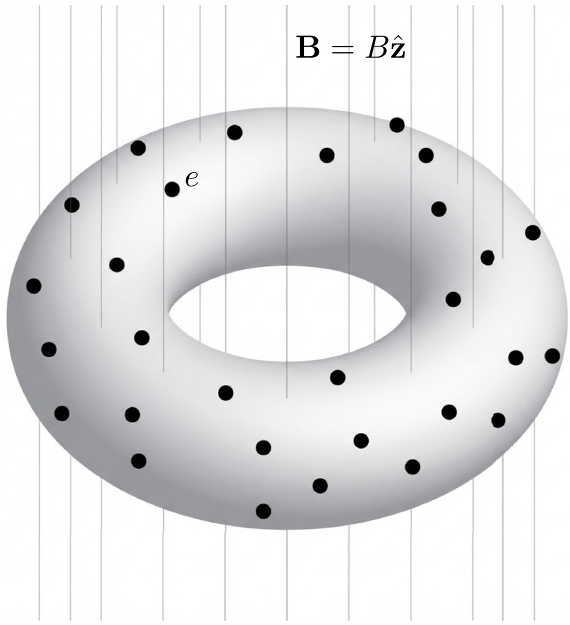

FIG. 1. Schematic of the fractional quantum Hall setup on a torus. N electrons (black dots) move on a two-dimensional torus with periodic boundary conditions and are subjected to a uniform perpendicular magnetic field $B\,\hat{\mathbf{z}}$.

III. CASE STUDY: FRACTIONAL QUANTUM HALL FLUID

Fractional quantum Hall (FQH) liquids provide a concrete setting where equilibrium, topology, transport, and strong correlations coexist in a highly constrained way. They occur for interacting electrons confined to two dimensions in a strong perpendicular magnetic field and were first observed in ultra-clean GaAs heterostructures through fractional plateaus of the Hall conductance and vanishing longitudinal resistance [59–61]. In this section we apply the above results to fractional quantum Hall systems and highlight two application-level points: (i) magnetic fields deform the shift algebra through an explicit density-weighted curvature insertion and (ii) in the lowest Landau level this deformation matches the guiding-center Girvin-MacDonald-Platzman (GMP) algebra.

A. Torus geometry, twists, and Hall topology

We consider N electrons (charge $q = -e$ and band mass m) confined to two dimensions and subject to a strong uniform perpendicular magnetic field $B\,\hat{\mathbf{z}}$ (Fig. 1). A standard continuum Hamiltonian is

$$\hat{H}_B = \sum_{a=1}^{N} \frac{1}{2m}[\hat{\mathbf{p}}_a - q\,\mathbf{A}(\hat{\mathbf{r}}_a)]^2 + \sum_{a<b} V(|\hat{\mathbf{r}}_a - \hat{\mathbf{r}}_b|) + \sum_a V_{\rm conf}(\hat{\mathbf{r}}_a), \tag{42}$$

with $\nabla \times \mathbf{A} = B\,\hat{\mathbf{z}}$. Here $V(r)$ is the two-body interaction potential, typically dominated by Coulomb repulsion or a short-range pseudopotential in model studies, and $V_{\rm conf}(\mathbf{r})$ is a one-body confining potential that enforces a finite droplet geometry when M has an edge; on the torus we set $V_{\rm conf} = 0$.

To isolate bulk constraints and eliminate boundary refinements of the shift algebra, we take

$$(x, y) \sim (x + L_x, y) \sim (x, y + L_y), \tag{43}$$

so $\partial M = \varnothing$. Here (x, y) are Cartesian coordinates on the covering space $\mathbb{R}^2$, and L_x and L_y are the linear periods of the torus in the x and y directions, respectively. In particular, the boundary term in the refined closure relation in Eq. (26) is absent. Throughout, all smearings and fields on $\mathbb{T}^2$ are taken to be smooth and periodic.

On $M = \mathbb{T}^2$ we implement twists (Aharonov-Bohm fluxes) by fixing the holonomies of an auxiliary flat background connection $\mathbf{A}_{\boldsymbol{\theta}}$ around the two fundamental cycles γ_x and γ_y. Here $\mathbf{A}_{\boldsymbol{\theta}}$ is a static $U(1)$ vector potential with vanishing field strength on M so it is locally pure gauge, but it carries nontrivial cycle integrals that implement the twist angles. Gauge invariantly, the twist sector $\boldsymbol{\theta} = (\theta_x, \theta_y) \in [0, 2\pi)^2$ is specified by

$$\nabla \times \mathbf{A}_{\boldsymbol{\theta}} = 0, \quad \exp\left[\frac{\mathrm{i}q}{\hbar}\oint_{\gamma_x} \mathbf{A}_{\boldsymbol{\theta}} \cdot d\mathbf{r}\right] = e^{\mathrm{i}\theta_x},$$
$$\exp\left[\frac{\mathrm{i}q}{\hbar}\oint_{\gamma_y} \mathbf{A}_{\boldsymbol{\theta}} \cdot d\mathbf{r}\right] = e^{\mathrm{i}\theta_y}. \tag{44}$$

Note that $\nabla \times \mathbf{A}_{\boldsymbol{\theta}} = 0$ means the twist does not change the local magnetic field strength; it only changes the global holonomy class and therefore the spectrum and eigenstates through boundary phases. In a convenient gauge this is equivalent to the familiar twisted boundary conditions on the many-body wave function, and the corresponding twisted Hamiltonian.

The twisted Hamiltonian in the sector $\boldsymbol{\theta}$ is obtained by coupling to the total background vector potential $\mathbf{A} + \mathbf{A}_{\boldsymbol{\theta}}$,

$$\hat{H}_{B,\boldsymbol{\theta}} = \hat{H}_B\Big|_{\mathbf{A}\,\to\,\mathbf{A}+\mathbf{A}_{\boldsymbol{\theta}}}, \tag{45}$$

where $H_{B,\boldsymbol{\theta}}$ is the many-body Hamiltonian with fixed magnetic field B and twist angles $\boldsymbol{\theta}$.

For a gapped ground state $|\Psi(\boldsymbol{\theta})\rangle$ of $H_{B,\boldsymbol{\theta}}$, the Niu-Thouless-Wu construction expresses the quantized Hall conductance as a Chern number over the twist torus $\boldsymbol{\theta} \in [0, 2\pi)^2$ [45,62,63]:

$$\sigma_{xy} = \frac{e^2}{h}C, \quad C = \frac{1}{2\pi}\int_0^{2\pi} d\theta_x \int_0^{2\pi} d\theta_y\, \Omega^{\rm B}_{\theta_x\theta_y}(\boldsymbol{\theta}), \tag{46}$$

where σ_{xy} is the zero-temperature dc Hall conductivity of the many-body ground state and $C \in \mathbb{Z}$ is the associated twist Chern number. Here $\Omega^{\rm B}_{\theta_x\theta_y} = \partial_{\theta_x}\mathfrak{M}_{\theta_y} - \partial_{\theta_y}\mathfrak{M}_{\theta_x}$ and $\mathfrak{M}_{\theta_j} = \mathrm{i}\langle\Psi(\boldsymbol{\theta})|\partial_{\theta_j}\Psi(\boldsymbol{\theta})\rangle$. Geometrically, $\mathfrak{M}$ is the Berry connection on the bundle of ground states over the twist torus, and $\Omega^{\rm B}$ is its Berry curvature.

B. Magnetic shift algebra as an inner curvature insertion

The following quantum-Hall construction specializes the general background-field deformation of Sec. II F to a two-dimensional torus. We set $M = \mathbb{T}^2$, take the only nonzero local field-strength component to be the uniform magnetic field $F^{\rm em}_{xy} = B$, and restrict to smooth periodic smearings. The flat twist connection $\mathbf{A}_{\boldsymbol{\theta}}$ defined in Eq. (44) changes the holonomy sector and hence the twisted Hamiltonian, but since $\nabla \times \mathbf{A}_{\boldsymbol{\theta}} = 0$ it does not change the local curvature insertion. The key structural input is therefore the same as in the general background-field case: minimal coupling makes covariant momenta noncommuting, so commuting two shift generators produces an explicit density insertion rather than a bulk central term. Define the magnetic shift generator for a smooth periodic vector field $\mathbf{f}(\mathbf{r})$ on $M = \mathbb{T}^2$ by

$$\hat{G}_B[\mathbf{f}] = \frac{1}{2}\sum_{a=1}^{N}[f^i(\hat{\mathbf{r}}_a)\,\hat{\pi}_{a,i} + \hat{\pi}_{a,i}\,f^i(\hat{\mathbf{r}}_a)]. \tag{47}$$

We write its adjoint derivation as

$$\Sigma_B[\mathbf{f}]\,X = -\frac{\mathrm{i}}{\hbar}\,[X, \hat{G}_B[\mathbf{f}]]. \tag{48}$$

A direct commutator calculation yields the deformed closure

$$[\hat{G}_B[\mathbf{f}], \hat{G}_B[\mathbf{g}]] = -\,\mathrm{i}\hbar\,\hat{G}_B[[\mathbf{f},\mathbf{g}]] + \mathrm{i}\hbar\,q\int_M d^2r\,f^i(\mathbf{r})\,g^j(\mathbf{r}) \times F^{\mathrm{em}}_{ij}(\mathbf{r})\,\hat{\rho}(\mathbf{r}). \tag{49}$$

Passing to adjoint actions, the deviation from Lie closure is an inner statistical-curvature insertion. Concretely, $\mathcal{F}_B(\mathbf{f},\mathbf{g})$ is the curvature functional of the magnetic shift derivations, defined by

$$\mathcal{F}_B(\mathbf{f},\mathbf{g}) = [\Sigma_B[\mathbf{f}], \Sigma_B[\mathbf{g}]] - \Sigma_B[[\mathbf{f},\mathbf{g}]],$$

so that $\mathcal{F}_B(\mathbf{f},\mathbf{g})[X]$ measures the failure of covariant Lie closure on any observable $X \in \mathfrak{A}_{\mathrm{obs}}$:

$$\mathcal{F}_B(\mathbf{f},\mathbf{g})[X] = \frac{\mathrm{i}}{\hbar}\Big[X,\ q\int_M d^2r\,f^i(\mathbf{r})g^j(\mathbf{r})\,F^{\mathrm{em}}_{ij}(\mathbf{r})\,\hat{\rho}(\mathbf{r})\Big]. \tag{50}$$

Thus Eqs. (49) and (50) are the quantum-Hall realization on the torus of the general curved-background algebra in Eq. (41).

Because the cocycle is inner, the Leibniz product rule is preserved and the Ward hierarchy can still be iterated; the only change relative to the flat bulk is the appearance of explicit density insertions in Bianchi-type compatibility relations.

C. Sector-resolved Ward-Bianchi hierarchy in the QH Gibbs state

For fixed twist $\boldsymbol{\theta}$, we work in the thermal state

$$\langle X\rangle_{B,\boldsymbol{\theta}} = \frac{\mathrm{Tr}\,(e^{-\beta\hat{H}_{B,\boldsymbol{\theta}}}\,X)}{Z_{B,\boldsymbol{\theta}}},\ \ Z_{B,\boldsymbol{\theta}} = \mathrm{Tr}\,(e^{-\beta\hat{H}_{B,\boldsymbol{\theta}}}). \tag{51}$$

Smearing the hyperforce identity (5) and using that $\Sigma_B[\mathbf{f}]$ is a derivation gives the QH Ward identity

$$\langle\Sigma_B[\mathbf{f}]\hat{A}\rangle_{B,\boldsymbol{\theta}} + (\hat{A}\,|\,F_{B,\boldsymbol{\theta}}[\mathbf{f}])_{B,\boldsymbol{\theta}} = 0,\ \ \forall\hat{A}\in\mathfrak{A}_{\mathrm{obs}}, \tag{52}$$

where the (dimensionless) smeared force insertion is

$$F_{B,\boldsymbol{\theta}}[\mathbf{f}] = -\Sigma_B[\mathbf{f}]\,\beta\hat{H}_{B,\boldsymbol{\theta}} = \int_M d^2r\,\mathbf{f}(\mathbf{r})\cdot\beta\hat{\mathbf{F}}_{B,\boldsymbol{\theta}}(\mathbf{r}). \tag{53}$$

Define the bilinear force-gradient kernel

$$K_{B,\boldsymbol{\theta}}[\mathbf{f},\mathbf{g}] = \Sigma_B[\mathbf{f}]\,F_{B,\boldsymbol{\theta}}[\mathbf{g}] = -\Sigma_B[\mathbf{f}]\Sigma_B[\mathbf{g}]\,\beta\hat{H}_{B,\boldsymbol{\theta}}. \tag{54}$$

Equations (53) and (54) are the sector-resolved analogs of Eqs. (30) and (31), with the replacements $\Sigma \to \Sigma_B$, $\hat{H}_0 \to \hat{H}_{B,\boldsymbol{\theta}}$, $F \to F_{B,\boldsymbol{\theta}}$, and $K_0 \to K_{B,\boldsymbol{\theta}}$. The Ward hierarchy keeps the same formal structure because the electromagnetic deformation in Sec. II F is inner and hence preserves the Leibniz product rule for the smeared shift derivation. Then, exactly as in the bulk-flat case, the all-orders closed Ward-Bianchi hierarchy holds for all $n \geqslant 2$:

$$\left(\prod_{j=1}^{n-1}F_{B,\boldsymbol{\theta}}[\mathbf{f}_j]\,\middle|\,F_{B,\boldsymbol{\theta}}[\mathbf{f}_n]\right)_{B,\boldsymbol{\theta}} + \sum_{k=1}^{n-1}\left\langle\prod_{j<k}F_{B,\boldsymbol{\theta}}[\mathbf{f}_j]\,K_{B,\boldsymbol{\theta}}[\mathbf{f}_n,\mathbf{f}_k] \times \prod_{j>k}F_{B,\boldsymbol{\theta}}[\mathbf{f}_j]\right\rangle_{B,\boldsymbol{\theta}} = 0. \tag{55}$$

The only formal change relative to the bulk-flat compatibility relation (35) appears in the Bianchi-type antisymmetry relation: inserting the inner curvature term inherited from Eq. (49) gives

$$K_{B,\boldsymbol{\theta}}[\mathbf{f},\mathbf{g}] - K_{B,\boldsymbol{\theta}}[\mathbf{g},\mathbf{f}] = F_{B,\boldsymbol{\theta}}[[\mathbf{f},\mathbf{g}]] + \beta\,q\int d^2r\,f^i(\mathbf{r})g^j(\mathbf{r}) \times F^{\mathrm{em}}_{ij}(\mathbf{r})\,\hat{\rho}(\mathbf{r}). \tag{56}$$

Mori positivity continues to provide a model-independent consistency and stability bound:

$$(F_{B,\boldsymbol{\theta}}[\mathbf{f}]\,|\,F_{B,\boldsymbol{\theta}}[\mathbf{f}])_{B,\boldsymbol{\theta}} = -\langle K_{B,\boldsymbol{\theta}}[\mathbf{f},\mathbf{f}]\rangle_{B,\boldsymbol{\theta}} \geqslant 0. \tag{57}$$

D. Lowest Landau level (LLL) reduction and the GMP-W_∞ dictionary

Equation (56) is a Ward-Bianchi consequence of the magnetic generator algebra in Eq. (49). The factor β in Eq. (56) comes only from the dimensionless definition $F_{B,\boldsymbol{\theta}} = -\Sigma_B\,\beta\hat{H}_{B,\boldsymbol{\theta}}$; the underlying algebraic deformation is the density-weighted curvature insertion $qF^{\mathrm{em}}_{ij}\hat{\rho}$. After projection to the LLL, the kinetic motion is quenched and the same curvature is represented by the noncommutative guiding-center density algebra.

With our sign convention, the guiding-center coordinates obey

$$\big[\hat{R}^x_a, \hat{R}^y_b\big] = -\mathrm{i}\,\ell_B^2\,\delta_{ab},$$

where $\hat{\mathbf{R}}_a$ is the guiding-center coordinate of particle a. The projected guiding-center density modes are

$$\bar{\rho}_{\mathbf{q}} = \sum_a \exp(\mathrm{i}\,\mathbf{q}\cdot\hat{\mathbf{R}}_a),$$

up to the standard scalar LLL form factor in the physical density mode, $\hat{\rho}^{\mathrm{LLL}}_{\mathbf{q}} = e^{-\ell_B^2|\mathbf{q}|^2/4}\bar{\rho}_{\mathbf{q}}$, which does not affect the closure algebra.

For a two-dimensional wave vector $\mathbf{q} = (q_x, q_y)$, and with $\ell_B = \sqrt{\hbar/|qB|}$, the Baker-Campbell-Hausdorff formula gives the standard Girvin-MacDonald-Platzman relation [64–66]

$$[\bar{\rho}_{\mathbf{q}}, \bar{\rho}_{\mathbf{q}'}] = 2\mathrm{i}\sin\Big(\frac{\ell_B^2}{2}(\mathbf{q}\times\mathbf{q}')_z\Big)\,\bar{\rho}_{\mathbf{q}+\mathbf{q}'}. \tag{58}$$

The connection with Eq. (56) is clearest in the long-wavelength expansion

$$[\bar{\rho}_{\mathbf{q}}, \bar{\rho}_{\mathbf{q}'}] = \mathrm{i}\,\ell_B^2(\mathbf{q}\times\mathbf{q}')_z\,\bar{\rho}_{\mathbf{q}+\mathbf{q}'} + O\big(\big[\ell_B^2(\mathbf{q}\times\mathbf{q}')_z\big]^3\big).$$

For a uniform field $F^{\rm em}_{xy} = B$, the contraction $f^i g^j F^{\rm em}_{ij} = B(f^x g^y - f^y g^x)$ is represented, for Fourier-labeled LLL generators, by the symplectic area factor $(\mathbf{q}\times\mathbf{q}')_z$, while the continuum density insertion $\hat{\rho}$ is replaced by the projected density mode $\bar{\rho}_{\mathbf{q}+\mathbf{q}'}$, up to form factors and normalization conventions. Thus Eq. (58) is the finite-$\mathbf{q}$, LLL-projected completion of the same curvature insertion that deforms the compatibility relation in Eq. (56).

This identification also explains the numerical implementation in Sec. IV A: the finite-torus Weyl operators $U_{m,n}$ are discrete representatives of $\exp(i\mathbf{q}\cdot\hat{\mathbf{R}})$, the many-body operators $\rho_{\mathbf{q}} = \mathsf{SQ}(U_{m,n})$ are the numerical analogs of $\bar{\rho}_{\mathbf{q}}$, and Eq. (60) is the finite-dimensional GMP algebra. The closure residual in Eq. (66) therefore tests the LLL realization of the curvature-deformed algebra, while the Hermitian sine generator $G_{\mathbf{q}}$ in Eq. (67) provides the projected representative of a smeared magnetic shift generator.

IV. NUMERICAL CALCULATION

A. Numerical methods

All numerics are exact diagonalization (ED) in fixed-N_e sectors, where $N_e = N$ is the total number of electrons. We use the occupation-number (Fock) basis $|n_0,\ldots,n_{N_{\rm orb}-1}\rangle$, where $N_{\rm orb}$ is the number of single-particle orbitals retained in the chosen finite-size geometry and $n_j \in \{0,1\}$ denotes the occupation of orbital j (so that $\sum_{j=0}^{N_{\rm orb}-1} n_j = N_e$). Basis states are encoded as bitstrings and fermionic signs in applying one-body bilinears $c_a^\dagger c_b$ are handled exactly, where c_b annihilates an electron in orbital b and $c_a^\dagger$ creates an electron in orbital a (so $c_a^\dagger c_b$ moves a particle from b to a). For the sizes used the fixed-N_e Hilbert-space dimension is $\binom{N_{\rm orb}}{N_e}$ (e.g. $\binom{11}{3} = 165$ and $\binom{9}{3} = 84$), so we form dense Hermitian matrices and diagonalize them directly.

The discretizations below test the analytical identities of Secs. II and III in a finite-dimensional LLL setting. The clock-shift algebra realizes the projected-density (GMP) algebra in Eq. (58); the closure defect in Eqs. (64)–(66) tests the absence of an additional bulk closure anomaly; the residual in Eq. (69) tests the thermal Ward identity in Eq. (52); and the twist-mesh construction in Eqs. (75)–(77) discretizes the Berry-curvature formula in Eq. (46).

On a magnetic torus with N_ϕ flux quanta, the one-body LLL Hilbert space has dimension N_ϕ. We use the standard $N_\phi\times N_\phi$ clock-shift pair $(\hat{C},\hat{S})$, where $\hat{C}$ is diagonal (the "clock") and $\hat{S}$ is the one-step cyclic translation (the "shift") in the LLL orbital index basis $\{|j\rangle\}_{j=0}^{N_\phi-1}$: $\hat{C}|j\rangle = \omega^j|j\rangle$ and $\hat{S}|j\rangle = |j+1\rangle$ (with wrap-around). They obey $\hat{S}^{N_\phi} = \hat{C}^{N_\phi} = \mathbb{1}$ and $\hat{C}\hat{S} = \omega\,\hat{S}\hat{C}$ with $\omega = e^{2\pi i/N_\phi}$. For odd N_ϕ we take $\tau = \exp\,(i\pi\frac{N_\phi+1}{N_\phi})$ and define the discrete Weyl operators

$$U_{m,n} = \tau^{mn}\hat{S}^m\hat{C}^n,\ \ (m,n)\in\mathbb{Z}^2_{N_\phi}, \tag{59}$$

which satisfy the projective commutator

$$\begin{aligned}[U_{m_1,n_1},U_{m_2,n_2}] &= (\tau^{\Delta}-\tau^{-\Delta})\,U_{m_1+m_2,\,n_1+n_2},\\ \Delta &\equiv n_1m_2 - m_1n_2,\end{aligned} \tag{60}$$

with all indices modulo N_ϕ.

Equation (60) is the finite-torus version of the LLL projected-density algebra in Eq. (58). The integer Δ is the discrete symplectic area of the two momentum labels, and the commutator closes on the combined label modulo N_ϕ. In the long-wavelength limit this is the projected-density realization of the density-weighted curvature insertion in Eq. (56).

We lift one-body matrices to the fixed-N_e many-body Hilbert space via the second-quantization map

$$\mathsf{SQ}(U) = \sum_{a,b=0}^{N_\phi-1} U_{ab}\,c_a^\dagger c_b, \tag{61}$$

and define the many-body guiding-center modes

$$\rho_{\mathbf{q}} = \mathsf{SQ}(U_{m,n}),\ \ \mathbf{q}=(m,n)\in\mathbb{Z}^2_{N_\phi}. \tag{62}$$

Thus $\rho_{\mathbf{q}}$ is the ED representative of the projected guiding-center density $\bar{\rho}_{\mathbf{q}}$ used in Eq. (58). The defect $D(\mathbf{q}_1,\mathbf{q}_2)$ below subtracts the exact right-hand side of the finite Weyl algebra in Eq. (60); consequently, $\epsilon_{\rm flat}$ measures the finite-torus version of the closure residual $[\Sigma[\mathbf{f}],\Sigma[\mathbf{g}]] - \Sigma[[\mathbf{f},\mathbf{g}]]$.

For the finite-temperature Ward test we use a translation-invariant projected density-density Hamiltonian

$$H = \sum_{\mathbf{q}\neq\mathbf{0}} V(\mathbf{q})\,\rho_{-\mathbf{q}}\rho_{\mathbf{q}}, \tag{63}$$

with $\rho_{-\mathbf{q}} = \rho_{\mathbf{q}}^\dagger$ and real $V(\mathbf{q})$ [we symmetrize $H\mapsto\frac{1}{2}(H+H^\dagger)$ in floating point]. For the finite-temperature Ward test, we take $V(\mathbf{q}) = e^{-\alpha|\mathbf{q}|^2}$ with $\alpha = 0.35$ and $|\mathbf{q}|^2 = \tilde{m}^2+\tilde{n}^2$, $\tilde{m} = \min(m, N_\phi - m)$, $\tilde{n} = \min(n, N_\phi - n)$. Unless stated otherwise, the LLL torus data use $N_\phi = 11$ and $N_e = 3$.

To test Lie closure we form the operator-level defect

$$D(\mathbf{q}_1,\mathbf{q}_2) = [\rho_{\mathbf{q}_1},\rho_{\mathbf{q}_2}] - (\tau^{\Delta_{12}}-\tau^{-\Delta_{12}})\,\rho_{\mathbf{q}_1+\mathbf{q}_2}, \tag{64}$$

where $\mathbf{q}_\ell = (m_\ell,n_\ell)\in\mathbb{Z}^2_{N_\phi}$ and

$$\Delta_{12} = n_1m_2 - m_1n_2 \pmod{N_\phi}, \tag{65}$$

and all additions $\mathbf{q}_1+\mathbf{q}_2$ are understood componentwise modulo N_ϕ. We quantify the defect by the dimensionless residual

$$\epsilon_{\rm flat}(\mathbf{q}_1,\mathbf{q}_2) = \frac{\|[X, D(\mathbf{q}_1,\mathbf{q}_2)]\|_{\rm HS}}{\|X\|_{\rm HS}}, \tag{66}$$

where X is a random Hermitian observable and $\|\cdot\|_{\rm HS}$ is the Hilbert-Schmidt norm.

A vanishing $\epsilon_{\rm flat}$ therefore means that, after subtracting the expected finite GMP-Weyl-algebra right-hand side, no additional bulk closure defect remains. When the wrap-around matrix element is removed in the open-chain surrogate, the same diagnostic probes the boundary-triggered failure mode associated with the boundary refinement in Eq. (26).

To test the finite-T hyperforce Ward identity we define, for each $\mathbf{q}$, the Hermitian sine generator

$$G_{\mathbf{q}} = \frac{1}{2i}(\rho_{\mathbf{q}} - \rho_{-\mathbf{q}}), \tag{67}$$

and (setting $\hbar = 1$) the adjoint derivation and force insertion

$$\Sigma[\mathbf{f}_{\mathbf{q}}]A = -i[A, G_{\mathbf{q}}],\ \ F[\mathbf{f}_{\mathbf{q}}] = -\Sigma[\mathbf{f}_{\mathbf{q}}]\,\beta\hat{H} = i\,\beta[\hat{H}, G_{\mathbf{q}}]. \tag{68}$$

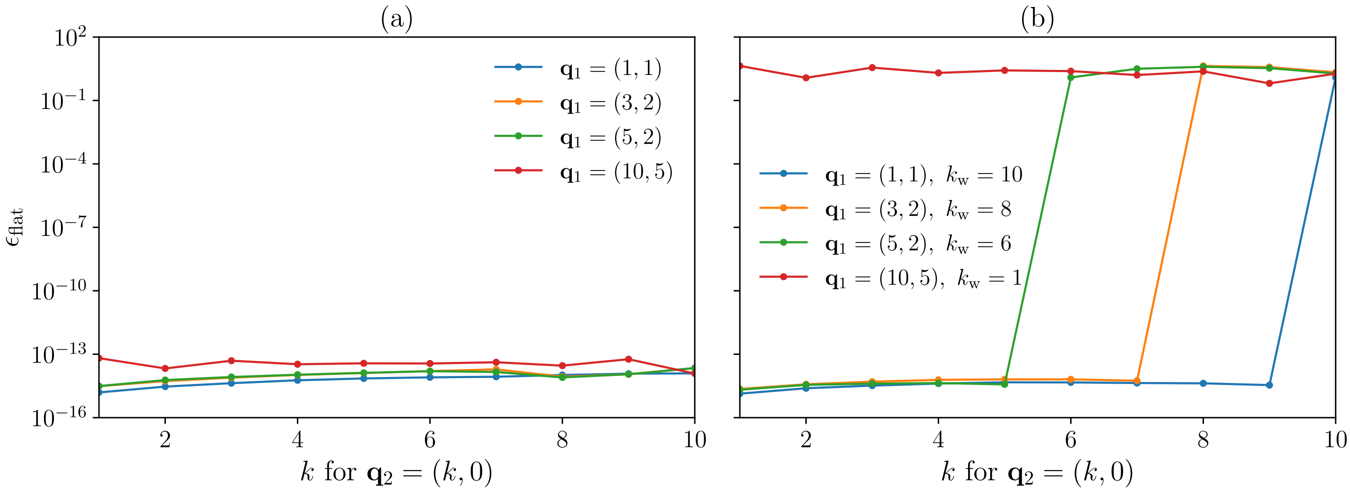

FIG. 2. Bulk Lie-closure diagnostic in the LLL torus model. We compute the residual $\epsilon_{\rm flat}(\mathbf{q}_1, \mathbf{q}_2)$ defined in Eqs. (64)–(66) using $\rho_{\mathbf{q}}$ on a torus with $N_\phi = 11$ and $N_e = 3$ [dim $\mathcal{H} = \binom{11}{3} = 165$]. We fix $\mathbf{q}_2 = (k, 0)$ and sweep $k = 1, \dots, N_\phi - 1$. (a) Periodic torus: The residual is at roundoff, confirming exact bulk closure. (b) Open-chain surrogate (wrap-around removed): The residual stays small up to the first wrapping step k_w and then jumps to order unity, demonstrating boundary-triggered violations. Here k_w denotes the smallest k for which the x-component addition in $\mathbf{q}_1 + \mathbf{q}_2$ requires the torus modular reduction (i.e., the first time the composed momentum wraps around the magnetic Brillouin zone in the x direction). For $\mathbf{q}_2 = (k, 0)$ this occurs at $k_w = N_\phi - q_{1x}$, with q_{1x} the first component of $\mathbf{q}_1$ (values indicated in the legend).

The Ward residual is

$$R_1(\mathbf{q}; \beta) = \langle \Sigma[\mathbf{f_q}] A \rangle_\beta + (A \mid F[\mathbf{f_q}])_\beta. \tag{69}$$

Equations (68) and (69) are the finite-dimensional counterparts of the definitions $F_{B,\boldsymbol{\theta}}[\mathbf{f}] = -\Sigma_B[\mathbf{f}]\, \beta \hat{H}_{B,\boldsymbol{\theta}}$ and of the Ward identity in Eq. (52), with the discrete Fourier label $\mathbf{q}$ replacing the continuum smearing field $\mathbf{f}$. Hence R_1 is a direct ED residual for the hyperforce Ward identity.

We evaluate $(A \mid F)_\beta$ exactly in the H eigenbasis using the closed spectral form

$$(A \mid F[\mathbf{f_q}])_\beta = \mathrm{i} \sum_{\alpha,\alpha'} (w_{\alpha'} - w_\alpha) A^*_{\alpha\alpha'} (G_{\mathbf{q}})_{\alpha\alpha'}, \quad w_{\alpha'} = \frac{e^{-\beta E_{\alpha'}}}{Z_\beta},$$

$$Z_\beta = \sum_\gamma e^{-\beta E_\gamma}, \quad H|\psi_{\alpha'}\rangle = E_{\alpha'}|\psi_{\alpha'}\rangle. \tag{70}$$

Here $\{|\psi_\alpha\rangle\}$ is a complete orthonormal set of many-body energy eigenstates of H in the fixed-N_e sector, $A_{\alpha\alpha'} = \langle\psi_\alpha|A|\psi_{\alpha'}\rangle$ and $(G_{\mathbf{q}})_{\alpha\alpha'} = \langle\psi_\alpha|G_{\mathbf{q}}|\psi_{\alpha'}\rangle$.

For each fixed finite torus the fixed-N_e Fock basis is complete and Eqs. (67)–(70) are identities between finite matrices. Indeed, using $F[f_{\mathbf{q}}] = \mathrm{i}\beta[\hat{H}, G_{\mathbf{q}}]$ gives

$$\langle \Sigma[f_{\mathbf{q}}] A \rangle_\beta = -\mathrm{i} \sum_{\alpha,\alpha'} (w_{\alpha'} - w_\alpha) A^*_{\alpha\alpha'} (G_{\mathbf{q}})_{\alpha\alpha'} = -(A \mid F[f_{\mathbf{q}}])_\beta. \tag{71}$$

Thus $R_1^{(N_\phi,N_e)}(\mathbf{q}; \beta) = 0$ in exact arithmetic for every N_ϕ, N_e, $\mathbf{q}$, and β. For the twist-holonomy test, we use a Hofstadter regularization on an $N_x \times N_y$ torus with flux ϕ per plaquette and twists $\boldsymbol{\theta} = (\theta_x, \theta_y)$. In Landau gauge,

$$h(\boldsymbol{\theta}) = -t \sum_{x,y} \big[e^{\mathrm{i}\theta_x \delta_{x,N_x-1}} c^\dagger_{x+1,y} c_{x,y} + e^{\mathrm{i}(2\pi\phi x + \theta_y \delta_{y,N_y-1})} \times c^\dagger_{x,y+1} c_{x,y} + \text{H.c.} \big], \tag{72}$$

where t is the nearest-neighbor hopping amplitude and the many-body Hamiltonian is obtained by the same second-quantization map as above,

$$H(\boldsymbol{\theta}) = \mathsf{SQ}(h(\boldsymbol{\theta})) = \sum_{\alpha,\alpha'} h_{\alpha\alpha'}(\boldsymbol{\theta})\, c^\dagger_\alpha c_{\alpha'}, \tag{73}$$

in the fixed-N_e sector. We compute the canonical free energy

$$\mathfrak{F}(\boldsymbol{\theta}) = -\frac{1}{\beta} \ln \mathrm{Tr}_{N_e}(e^{-\beta \hat{H}(\boldsymbol{\theta})}), \tag{74}$$

and a current proxy $I_x(\boldsymbol{\theta}) \propto -\partial_{\theta_x}\mathfrak{F}(\boldsymbol{\theta})$ by finite differences. At $T = 0$ we compute the twist Chern number using the Fukui-Hatsugai-Suzuki link variables

$$U_x(i, j) = \frac{\langle\Psi_{i,j}|\Psi_{i+1,j}\rangle}{|\langle\Psi_{i,j}|\Psi_{i+1,j}\rangle|}, \quad U_y(i, j) = \frac{\langle\Psi_{i,j}|\Psi_{i,j+1}\rangle}{|\langle\Psi_{i,j}|\Psi_{i,j+1}\rangle|}, \tag{75}$$

Here $|\Psi_{i,j}\rangle$ is the normalized many-body ground state of $H(\theta_x^{(i)}, \theta_y^{(j)})$ at the twist-mesh point $(\theta_x^{(i)}, \theta_y^{(j)})$.

The plaquette curvature

$$F_{ij} = \mathrm{Arg}[U_x(i, j)\, U_y(i+1, j)\, U_x(i, j+1)^{-1}\, U_y(i, j)^{-1}], \tag{76}$$

and

$$C = \frac{1}{2\pi} \sum_{i,j} F_{ij}. \tag{77}$$

These link variables are the lattice discretization of the Berry connection on the twist torus. The plaquette phase F_{ij} is the discrete Berry curvature entering the Niu-Thouless-Wu formula in Eq. (46); the sum in Eq. (77) therefore gives the finite-mesh version of the twist-sector Chern number and implements the holonomy discussion of Sec. II E.

We use $N_x = N_y = 3$, $\phi = 1/3$, $t = 1$, $N_e = 3$, and a 15×15 twist mesh.

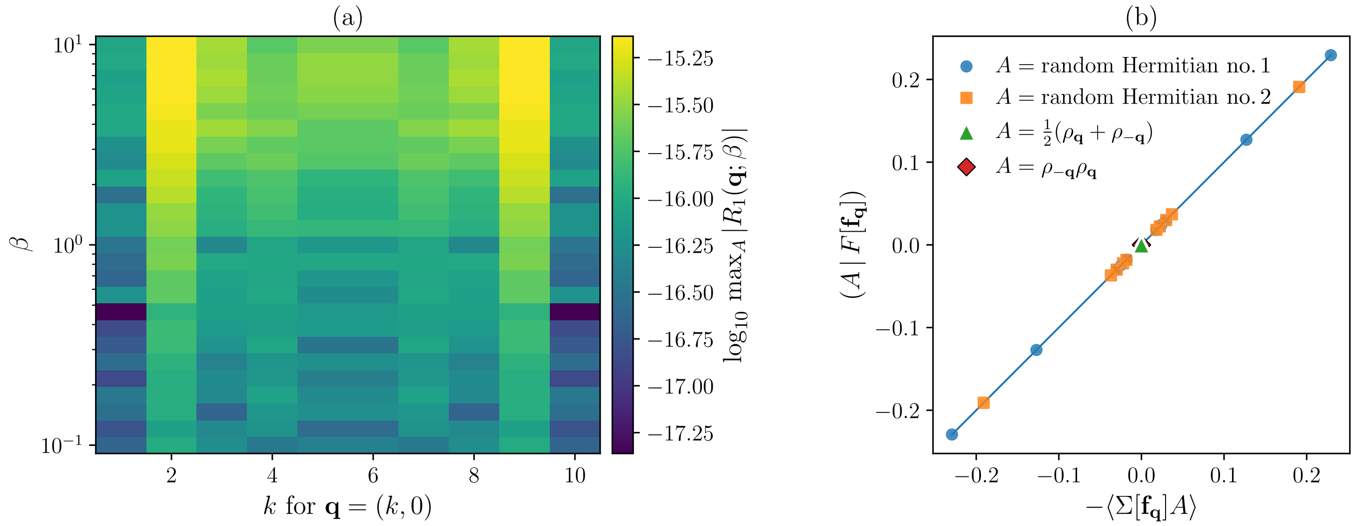

FIG. 3. Finite-temperature ED verification of the hyperforce Ward identity in the LLL torus model. We use $N_\phi = 11$, $N_e = 3$, and the translation-invariant Hamiltonian (63) with $V(\mathbf{q}) = e^{-\alpha|\mathbf{q}|^2}$ and $\alpha = 0.35$. For $\mathbf{q} = (k, 0)$ we evaluate the Ward residual $R_1(\mathbf{q}; \beta)$ in Eq. (69), with the Kubo-Mori term computed from the exact spectral formula (70). (a) Error map of $\log_{10} \max_A |R_1|$ over (k, β). (b) Parity plot at $\beta = 2$ comparing $(A \mid F)_\beta$ versus $-\langle \Sigma A \rangle_\beta$; the diagonal is the Ward prediction.

B. Numerical results

Figure 2(a) shows the periodic-torus result, where ϵ_{flat} remains at double-precision roundoff across all sampled momenta, confirming that the many-body $\rho_{\mathbf{q}}$ inherit exact closure from the finite-dimensional Weyl algebra. This is the discrete ED analog of "no bulk anomaly": there is no systematic growth with momentum or choice of $\mathbf{q}_1$, only numerical noise. In contrast, Fig. 2(b) shows the open-chain surrogate. By removing the wrap-around matrix element in the one-body shift, the only way to violate closure is to force an operation that would have crossed the boundary. The residual indeed remains at roundoff until the first wrapping index and then jumps to order unity. This isolates the failure mode as boundary-triggered rather than diffuse, matching the boundary-refined closure logic used in the continuum discussion.

Figure 3 tests the finite-temperature hyperforce Ward identity. Figure 3(a) shows that the worst-case residual $\max_A |R_1(q; \beta)|$ stays at roundoff across both wave vector and temperature, even though the two Ward terms being compared are individually not small. The parity plot in Fig. 3(b) makes the cancellation transparent: for a fixed β and a range of momenta, $(A \mid F)_\beta$ collapses onto $-\langle \Sigma A \rangle_\beta$ for both generic

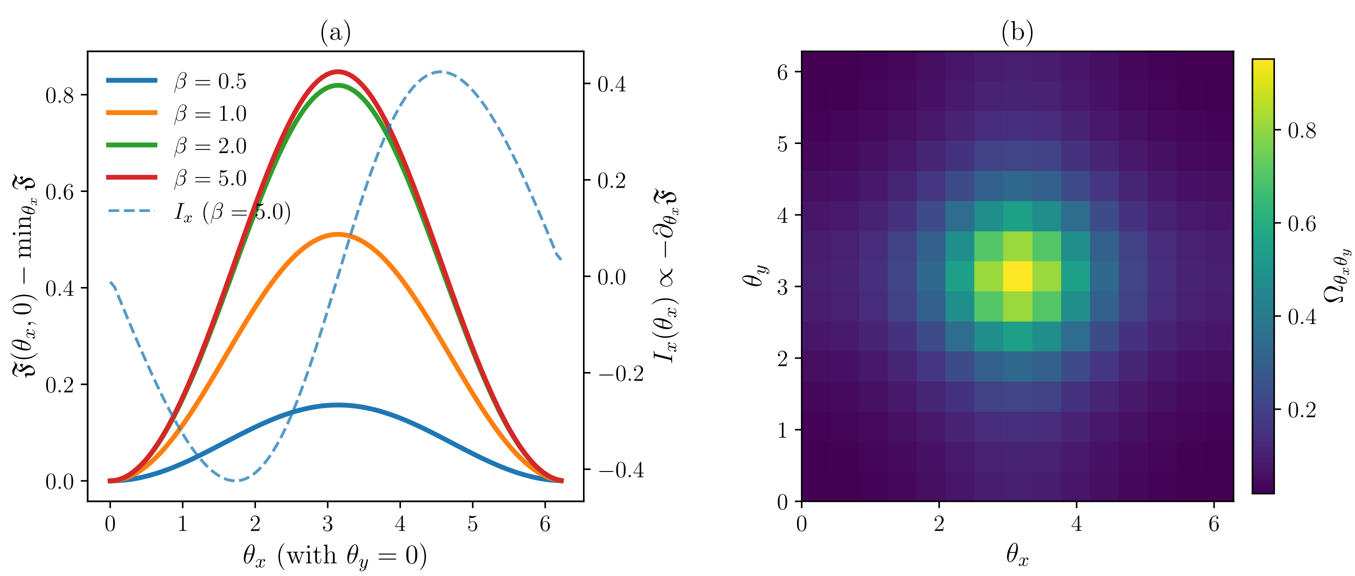

FIG. 4. Flux-threading-holonomy spectroscopy on the twist torus. We diagonalize the fixed-N_e Hofstadter family $H(\theta_x, \theta_y) = \mathsf{SQ}(h(\theta_x, \theta_y))$ [Eqs. (72)–(73)] on an $N_x \times N_y$ torus. Parameters: $N_x = N_y = 3$, $\phi = 1/3$, $t = 1$, and $N_e = 3$ [dim $\mathcal{H} = \binom{9}{3} = 84$]. (a) Canonical free energy $\mathfrak{F}(\theta_x, 0)$ from Eq. (74), shown relative to its minimum, for $\beta = \{0.5, 1, 2, 5\}$, together with the current proxy $I_x(\theta_x) \propto -\partial_{\theta_x}\mathfrak{F}$ at $\beta = 5$. (b) Ground-state Berry curvature density on a 15×15 twist mesh computed with the FHS method [Eqs. (75)–(77)]; the integrated Chern number is $C \simeq 1$.

random observables and structured density operators. In this sense the test is stringent: it does not merely show that the residual is small, but that two independently computed quantities (a commutator expectation value and a Kubo-Mori inner product) track each other in sign and magnitude. The finite-size dependence of the algebraic residual is therefore simple: increasing N_ϕ changes the number of available magnetic Fourier modes and the Hilbert-space dimension, but it does not introduce a systematic Ward-identity error to be extrapolated. On the periodic torus the closure defect and R_1 vanish size by size in exact arithmetic; hence their numerical values are expected to remain pinned near machine precision, rather than decay exponentially with N_ϕ. The inverse temperature β changes the Gibbs weights and the magnitude of the two canceling terms in Eq. (71); it does not affect the exact cancellation. For a gapped spectrum, thermal observables approach their ground-state values as $O(e^{-\beta\Delta})$, whereas the Ward hierarchy holds at every finite β.

Figure 4 demonstrates the complementary "global" diagnostic: even when the twist background is locally flat, the holonomy angles (θ_x, θ_y) produce measurable spectral flow, equilibrium currents, and Berry phases. Figure 4(a) shows that, along the cut $\theta_y = 0$, the free energy $\mathfrak{F}(\theta_x, 0)$ is 2π-periodic, and its twist dependence grows as β increases because the free energy crosses over from a thermally averaged quantity to the ground-state energy. The current proxy $I_x \propto -\partial_{\theta_x}\mathfrak{F}$ vanishes at extrema and reverses sign across $\theta_x \simeq \pi$, giving a directly interpretable holonomy response. Figure 4(b) shows the same physics in topological form: the Berry curvature density on the twist torus is nonuniform at small system size, but its integral yields an integer Chern number.

V. CONCLUSION AND OUTLOOK

In this work we formulated quantum shift symmetry in equilibrium as a statistical-gauge geometry on the observable bundle over configuration space. Starting from the exact hyperforce identity (5), we reinterpreted the local shifting superoperator as a derivation-valued connection and identified the corresponding hyperforces as covariant derivatives. This geometric packaging makes two structural issues transparent that are otherwise obscured by the distributional character of local currents: (i) whether the shift algebra closes without a bulk anomaly and (ii) whether the resulting Ward identities can be iterated to yield a closed hierarchy of equal-time constraints.

Our first main result is distributional bulk flatness for compact smearings, expressed by the covariant Lie-closure relation (21), equivalently by the smeared relation (29). In particular, successive shift variations close on the Lie bracket of vector fields with no bulk Schwinger term, so the statistical connection has vanishing bulk curvature in the distributional sense. This is precisely the input needed for iteration: together with the Leibniz product rule on a unital observable algebra, bulk flatness yields an all-orders closed Ward-Bianchi hierarchy for smeared force insertions, Eq. (32), which terminates on the bilinear force-gradient kernel and generates no new bulk insertions at higher order. Immediate corollaries include antisymmetry Bianchi-type compatibility relations and model-independent positivity and stability bounds rooted in the Kubo-Mori inner product.

Our second main result fixes the microscopic generator ordering and explains the absence of bulk ordering anomalies. By quantizing the diffeomorphism moment map (fiber-linear in momenta), Weyl and half-density quantization select the unique self-adjoint shift generator compatible with unitary diffeomorphism implementation. Because the underlying symbols are momentum-linear, the would be $\hbar^2$ ordering ambiguities that obstruct general quantization maps do not appear here, and the generator algebra closes exactly at the quantum level. In this sense, the geometric viewpoint not only reproduces the known quantum hyperforce identity, but also isolates the minimal structural ingredients required for a closed and anomaly-free bulk hierarchy.

Although local curvature invariants vanish in the bulk-flat case, global topology survives through holonomy. We showed that inequivalent unitary lifts of the adjoint holonomy are classified by $U(1)$ characters, equivalently by first cohomology with unitary coefficients, Eq. (39). This provides a direct bridge between statistical-gauge geometry and standard finite-size and topological diagnostics: twisted boundary conditions, flux threading, and twist-torus Berry phases can be recast as probes of flat holonomy sectors via thermal Wilson characters and twisted traces. The resulting character grading yields sharp selection rules for equilibrium one- and many-point functions in monodromy-invariant KMS states.

Coupling to a background electromagnetic field deforms the shift algebra in a way that is conceptually clean: the deformation is an inner curvature insertion proportional to the density and field strength, Eq. (41), rather than a bulk central extension. This preserves the derivation structure, equivalently the Leibniz product rule, and therefore preserves the iterability of the Ward-Bianchi hierarchy, while making explicit how local curvature and global holonomy effects separate. In the fractional quantum Hall case study on the torus, this mechanism connects naturally to the guiding-center noncommutative geometry and the GMP-W_∞ structure, yielding sector-resolved equilibrium constraints under flux threading. Our exact diagonalization tests provide concrete diagnostics of the framework: bulk Lie closure at the operator level, finite-T verification of the hyperforce Ward identity, and global holonomy spectroscopy on the twist torus.

Several extensions are immediate. A systematic boundary formulation is needed. Bulk flatness holds for compact smearings, but boundaries and noncompact smearings generate surface-supported terms that can reorganize the Ward-Bianchi iteration. In quantum Hall settings this should provide a unified account of bulk constraints and universal edge physics. It is also important to generalize the construction to broader background geometries and additional conserved currents. Beyond the mass-current shift sector and its electromagnetic deformation, coupling to nonrelativistic spacetime geometry, such as Newton-Cartan structure [40,67] with possible torsion and local rotations, should place momentum and stress on the same geometric footing. This direction is expected to yield new exact equal-time constraints, including mixed relations involving currents and stress.

A further direction is to move beyond equilibrium [68]. Since the hyperforce identity is rooted in operator algebra and the KMS condition, it should admit controlled extensions to slowly driven local Gibbs protocols [69,70], Keldysh formulations [71,72], and weakly nonequilibrium steady states [73,74]. In that setting it is natural to seek a response connection whose curvature measures the obstruction to iterating Ward identities away from equilibrium.

Finally, the closed hierarchy and its positivity consequences provide stringent, model-independent unit tests for numerics. They also suggest practical estimators for integrated force-gradient kernels and response data, including in topological phases where holonomy is essential. More broadly, the statistical-gauge viewpoint suggests that many equilibrium constraints are governed by a flat but globally nontrivial connection, with curvature activated only by boundaries or by genuine background field strength.

DATA AVAILABILITY

The code used to support the findings of this article is openly available [75].

[1] H. B. Callen and T. A. Welton, Irreversibility and generalized noise, Phys. Rev. **83**, 34 (1951).

[2] R. Kubo, Statistical-mechanical theory of irreversible processes. I. General theory and simple applications to magnetic and conduction problems, J. Phys. Soc. Jpn. **12**, 570 (1957).

[3] R. Kubo, The fluctuation-dissipation theorem, Rep. Prog. Phys. **29**, 255 (1966).

[4] H. Mori, Transport, collective motion, and Brownian motion, Prog. Theor. Phys. **33**, 423 (1965).

[5] R. Zwanzig, Memory effects in irreversible thermodynamics, Phys. Rev. **124**, 983 (1961).

[6] R. Kubo, M. Toda, and N. Hashitsume, *Statistical Physics II: Nonequilibrium Statistical Mechanics*, Springer Series in Solid-State Sciences, Vol. 31 (Springer, Berlin, 1991).

[7] G. D. Mahan, *Many-Particle Physics*, 3rd ed. (Kluwer Academic/Plenum Publishers, New York, 2000).

[8] D. Forster, *Hydrodynamic Fluctuations, Broken Symmetry, and Correlation Functions* (CRC Press, Boca Raton, FL, 2018).

[9] J. C. Ward, An identity in quantum electrodynamics, Phys. Rev. **78**, 182 (1950).

[10] Y. Takahashi, On the generalized Ward identity, Nuovo Cim. **6**, 371 (1957).

[11] L. P. Kadanoff and P. C. Martin, Hydrodynamic equations and correlation functions, Ann. Phys. **24**, 419 (1963).

[12] J.-y. Choi, S. Hild, J. Zeiher, P. Schauß, A. Rubio-Abadal, T. Yefsah, V. Khemani, D. A. Huse, I. Bloch, and C. Gross, Exploring the many-body localization transition in two dimensions, Science **352**, 1547 (2016).

[13] M. Yan, H.-Y. Hui, M. Rigol, and V. W. Scarola, Equilibration dynamics of strongly interacting bosons in 2D lattices with disorder, Phys. Rev. Lett. **119**, 073002 (2017).

[14] P. Bordia, H. Lüschen, S. Scherg, S. Gopalakrishnan, M. Knap, U. Schneider, and I. Bloch, Probing slow relaxation and many-body localization in two-dimensional quasiperiodic systems, Phys. Rev. X **7**, 041047 (2017).

[15] M. Yan, H.-Y. Hui, and V. W. Scarola, Dynamics of disordered states in the Bose–Hubbard model with confinement, Phys. Rev. A **95**, 053624 (2017).

[16] J.-P. Hansen and I. R. McDonald, *Theory of Simple Liquids: With Applications to Soft Matter*, 4th ed. (Academic Press, Oxford, 2013).

[17] P. M. Chaikin and T. C. Lubensky, *Principles of Condensed Matter Physics* (Cambridge University Press, Cambridge, 1995).

[18] R. Evans, The nature of the liquid-vapour interface and other topics in the statistical mechanics of non-uniform, classical fluids, Adv. Phys. **28**, 143 (1979).

[19] P. A. Martin, Sum rules in charged fluids, Rev. Mod. Phys. **60**, 1075 (1988).

[20] N. Nguyen-Tran-Thanh, T. Nguyen-Xuan, and H. Pham-Van, Gauge theory of orientation in anisotropic fluids, Phys. Rev. E **113**, 025401 (2026).

[21] S. Hermann and M. Schmidt, Noether's theorem in statistical mechanics, Commun. Phys. **4**, 176 (2021).

[22] S. Hermann and M. Schmidt, Why Noether's theorem applies to statistical mechanics, J. Phys.: Condens. Matter **34**, 213001 (2022).

[23] S. Hermann and M. Schmidt, Variance of fluctuations from Noether invariance, Commun. Phys. **5**, 276 (2022).

[24] F. Sammüller, S. Hermann, D. de las Heras, and M. Schmidt, Noether-constrained correlations in equilibrium liquids, Phys. Rev. Lett. **130**, 268203 (2023).

[25] S. Robitschko, F. Sammüller, M. Schmidt, and S. Hermann, Hyperforce balance via thermal Noether invariance of any observable, Commun. Phys. **7**, 103 (2024).

[26] S. Hermann, F. Sammüller, and M. Schmidt, Noether invariance theory for the equilibrium force structure of soft matter, J. Phys. A: Math. Theor. **57**, 175001 (2024).

[27] J. Müller, S. Hermann, F. Sammüller, and M. Schmidt, Gauge invariance of equilibrium statistical mechanics, Phys. Rev. Lett. **133**, 217101 (2024).

[28] J. Müller, F. Sammüller, and M. Schmidt, Why gauge invariance applies to statistical mechanics, J. Phys. A: Math. Theor. **58**, 125003 (2025).

[29] J. Matthes, S. Robitschko, J. Müller, S. Hermann, F. Sammüller, and M. Schmidt, Gauge invariance and hyperforce correlation theory for equilibrium fluid mixtures, J. Chem. Phys. **164**, 044903 (2026).

[30] H. Pham-Van, Unified gauge-geometry symmetry for equilibrium statistical mechanics, Phys. Rev. E **113**, 054134 (2026).

[31] D. de las Heras and M. Schmidt, Better than counting: Density profiles from force sampling, Phys. Rev. Lett. **120**, 218001 (2018).

[32] J. Renner, M. Schmidt, and D. de las Heras, Reduced-variance orientational distribution functions from torque sampling, J. Phys.: Condens. Matter **35**, 235901 (2023).

[33] J. Schwinger, Euclidean quantum electrodynamics, Phys. Rev. **115**, 721 (1959).

[34] D. G. Boulware and S. Deser, Stress-tensor commutators and Schwinger terms, J. Math. Phys. **8**, 1468 (1967).
[35] K. Jensen, Anomalies for Galilean fields, SciPost Phys. **5**, 005 (2018).
[36] A. Jain, Galilean anomalies and their effect on hydrodynamics, Phys. Rev. D **93**, 065007 (2016).
[37] K. Fernandes and A. Mitra, Gravitational anomalies on the Newton-Cartan background, Phys. Rev. D **96**, 085003 (2017).
[38] D. T. Son and M. Wingate, General coordinate invariance and conformal invariance in nonrelativistic physics: Unitary Fermi gas, Ann. Phys. **321**, 197 (2006).
[39] D. T. Son, Newton–Cartan geometry and the quantum Hall effect, Low Temp. Phys. **51**, 384 (2025).
[40] G. Festuccia, D. Hansen, J. Hartong, and N. A. Obers, Torsional Newton-Cartan geometry from the Noether procedure, Phys. Rev. D **94**, 105023 (2016).
[41] N. Banerjee, J. Bhattacharya, S. Bhattacharyya, S. Jain, S. Minwalla, and T. Sharma, Constraints on fluid dynamics from equilibrium partition functions, J. High Energy Phys. 09 (2012) 046.
[42] K. Jensen, M. Kaminski, P. Kovtun, R. Meyer, A. Ritz, and A. Yarom, Towards hydrodynamics without an entropy current, Phys. Rev. Lett. **109**, 101601 (2012).
[43] K. Jensen, R. Loganayagam, and A. Yarom, Thermodynamics, gravitational anomalies and cones, J. High Energy Phys. 02 (2013) 088.
[44] M. V. Berry, Quantal phase factors accompanying adiabatic changes, Proc. R. Soc. Lond. A. **392**, 45 (1984).
[45] Q. Niu, D. J. Thouless, and Y.-S. Wu, Quantized Hall conductance as a topological invariant, Phys. Rev. B **31**, 3372 (1985).
[46] J. Müller and M. Schmidt, Quantum statistical mechanical gauge invariance, arXiv:2509.20494.
[47] M. J. Gotay, On the Groenewold–van Hove problem for $\mathbb{R}^{2n}$, J. Math. Phys. **40**, 2107 (1999).
[48] M. J. Gotay, H. B. Grundling, and G. M. Tuynman, Obstruction results in quantization theory, J. Nonlinear Sci. **6**, 469 (1996).
[49] M. A. de Gosson, Bypassing the Groenewold–van Hove obstruction on $\mathbb{R}^{2n}$: A new argument in favor of Born–Jordan quantization, J. Phys. A: Math. Theor. **49**, 39LT01 (2016).
[50] G. B. Folland, *Harmonic Analysis in Phase Space*, Annals of Mathematics Studies, Vol. 122 (Princeton University Press, Princeton, NJ, 1989).
[51] B. C. Hall, *Quantum Theory for Mathematicians*, Graduate Texts in Mathematics, Vol. 267 (Springer, New York, 2013).
[52] N. M. J. Woodhouse, *Geometric Quantization*, 2nd ed. (Clarendon Press, Oxford, 1991).
[53] S. Kobayashi and K. Nomizu, *Foundations of Differential Geometry*, Vol. 2 (John Wiley & Sons, New York, 1996).
[54] M. Nakahara, *Geometry, Topology and Physics*, 2nd ed. (Taylor & Francis, Boca Raton, FL, 2003).
[55] J. M. Lee, *Introduction to Smooth Manifolds*, 2nd ed., Graduate Texts in Mathematics, Vol. 218 (Springer, New York, 2013).
[56] *Quantum Mechanics in Phase Space: An Overview with Selected Papers*, edited by C. K. Zachos, D. B. Fairlie, and T. L. Curtright (World Scientific, Singapore, 2005).
[57] R. Bott and L. W. Tu, *Differential Forms in Algebraic Topology*, Graduate Texts in Mathematics, Vol. 82 (Springer, New York, 1982).
[58] A. Hatcher, *Algebraic Topology* (Cambridge University Press, Cambridge, 2002).
[59] D. C. Tsui, H. L. Stormer, and A. C. Gossard, Two-dimensional magnetotransport in the extreme quantum limit, Phys. Rev. Lett. **48**, 1559 (1982).
[60] H. L. Stormer, Nobel lecture: The fractional quantum Hall effect, Rev. Mod. Phys. **71**, 875 (1999).
[61] H. L. Stormer, D. C. Tsui, and A. C. Gossard, The fractional quantum Hall effect, Rev. Mod. Phys. **71**, S298 (1999).
[62] N. Byers and C. N. Yang, Theoretical considerations concerning quantized magnetic flux in superconducting cylinders, Phys. Rev. Lett. **7**, 46 (1961).
[63] R. B. Laughlin, Quantized Hall conductivity in two dimensions, Phys. Rev. B **23**, 5632 (1981).
[64] S. M. Girvin and T. Jach, Formalism for the quantum Hall effect: Hilbert space of analytic functions, Phys. Rev. B **29**, 5617 (1984).
[65] S. M. Girvin, A. H. MacDonald, and P. M. Platzman, Collective-excitation gap in the fractional quantum Hall effect, Phys. Rev. Lett. **54**, 581 (1985).
[66] S. M. Girvin, A. H. MacDonald, and P. M. Platzman, Magnetoroton theory of collective excitations in the fractional quantum Hall effect, Phys. Rev. B **33**, 2481 (1986).
[67] M. Geracie, D. T. Son, C. Wu, and S.-F. Wu, Spacetime symmetries of the quantum Hall effect, Phys. Rev. D **91**, 045030 (2015).
[68] J. Müller, F. Sammüller, and M. Schmidt, Dynamical gauge invariance of statistical mechanics, arXiv:2504.17599.
[69] M. Hongo and K. Hattori, Revisiting relativistic magnetohydrodynamics from quantum electrodynamics, J. High Energy Phys. 02 (2021) 011.
[70] J. Mabillard and P. Gaspard, Quantum local-equilibrium approach to dissipative hydrodynamics, Phys. Rev. E **107**, 014102 (2023).
[71] L. M. Sieberer, M. Buchhold, J. Marino, and S. Diehl, Universality in driven open quantum matter, Rev. Mod. Phys. **97**, 025004 (2025).
[72] F. M. Haehl, R. Loganayagam, and M. Rangamani, Effective action for relativistic hydrodynamics: Fluctuations, dissipation, and entropy inflow, J. High Energy Phys. 10 (2018) 194.
[73] A. Levy, E. Rabani, and D. T. Limmer, Response theory for nonequilibrium steady states of open quantum systems, Phys. Rev. Res. **3**, 023252 (2021).
[74] G. Guarnieri, G. T. Landi, S. R. Clark, and J. Goold, Thermodynamics of precision in quantum nonequilibrium steady states, Phys. Rev. Res. **1**, 033021 (2019).
[75] H. Pham-Van, Code for "quantum statistical-gauge geometry", Zenodo, 2026, https://doi.org/10.5281/zenodo.20503382.